Journal of Sound and Vibration 328 (2009) 467–487

Contents lists available at ScienceDirect

Journal of Sound and Vibration

journal homepage: www.elsevier.com/locate/jsvi

Stability and free vibration analyses of an orthotropic singly symmetric Timoshenko beam-column with generalized end conditions

J.F. Monsalve-Cano [a], J. Darío Aristizábal-Ochoa [b,*]

[a] ACCIONA, Madrid, Spain
[b] School of Mines, National University of Colombia at Medellín, Colombia

ARTICLE INFO

Article history:
Received 1 February 2008
Received in revised form
14 August 2009
Accepted 17 August 2009
Handling Editor: C.L. Morfey
Available online 22 September 2009

ABSTRACT

The stability and free vibration analyses (i.e., buckling, natural frequencies and modal shapes) of an orthotropic singly symmetric 3D Timoshenko beam-column with generalized boundary conditions (i.e., with bending and torsional semirigid restraints and lateral bracings as well as lumped masses at both ends) subjected to an eccentric end axial load are presented in a classical manner. The five governing equations of dynamic equilibrium (i.e., two transverse shear equations, two bending moment equations and pure torsional moment equation) are sufficient to determine the natural frequencies and the corresponding modal shapes of the beam-column in the two principal planes of bending and torsion about its longitudinal axis. The proposed model includes the coupling effects among: (1) the deformations due to bending, shear and pure torsion; (2) inertias (translational, rotational and torsional) of all masses considered; (3) eccentric axial loads applied at the ends, and (4) restraints at the supports (bending, torsional and lateral bracings at both ends of the member). However, the effects of axial deformations and warping torsion produced by the axial load are not included; consequently the proposed model is not capable of capturing the phenomena of torsional buckling or combined lateral bending–torsional buckling. The proposed analytical model indicates that the stability and dynamic response of beam-columns are highly sensitive to the coupling effects, particularly in members with both ends free to rotate. The natural frequencies and modal shapes can be determined from the eigenvalues of a full 4×4 matrix for vibration in the plane of symmetry (using the uncoupled equations of transverse force and moment equilibrium at both ends) and from a full 6×6 matrix for the coupled shear–bending–torsional vibration (using the coupled equations of transverse shear, bending and torsional moment equilibrium at both ends). Also, it is shown that the proposed method reproduces the phenomena of modal interchanges (e.g. the second mode becoming the first mode and vise versa, etc.) when the bending and torsional restraints at the ends of the beam-column become very low. Four illustrative examples are presented showing the advantages and limitations of the proposed method.

* Corresponding author.
E-mail address: jdaristi2@yahoo.com (J. Darío Aristizábal-Ochoa).

0022-460X/$ - see front matter © 2009 Elsevier Ltd. All rights reserved.
doi:10.1016/j.jsv.2009.08.015

Nomenclature

A cross-sectional area of the beam-column
A_{sx} and A_{sy} effective shear areas along the x- and y-axes, respectively
A_1, A_2, A_3, A_4, A_5 and A_6 constants required in the vibration analysis of the beam-column in the yz-plane
E_z elastic modulus of the beam-column along the z-axis
F_1, F_2, F_3 and F_4 constants required in the vibration analysis of the beam-column in the xz-plane
G_x and G_y transverse shear moduli of the beam-column along the x- and y-axes, respectively
G_{xy} shear modulus of the beam-column under torsion
H_x and H_y shear force along the member in the x- and y-directions, respectively
I_α torsional inertia per unit of length of the beam-column about z-axis
I_x and I_y second moment of area of the beam-column cross section about the x-axis
J torsional moment of inertia of the cross section of the beam-column
J_{ax}, J_{ay} and J_{bx}, J_{by} rotational inertias of the masses at ends A and B about the x- and y-axes, respectively
$J_{a\psi}$ and $J_{b\psi}$ torsional inertias of the attached masses at ends A and B about the z-axis, respectively
$\overline{m}$ mass per unit length of the beam-column
$\overline{m}L^2r_x^2$ and $\overline{m}L^2r_y^2$ rotatory inertias of the beam column about the x- and y-axes, respectively
M_a and M_b rigid masses attached at the top and bottom ends of the beam-column, respectively
$M_x(\xi)$ and $M_y(\xi)$ bending moment along the beam-column about the x- and y-axes, respectively
L span of the beam-column
P end axial load applied at the centroid of the cross section with coordinates (x_α, 0); tensile positive
S_{ax}, S_{ay} and S_{bx}, S_{by} stiffness of the lateral bracings at ends A and B along the x- and y-axes, respectively
t time
T torsional moment
$u(z, t)$ lateral deflection of the shear center of the member along the x-axis
$v(z, t)$ lateral deflection of the shear center of the member along the y-axis
v_α lateral deflection of the centroidal line of the member along the y-axis
z centroidal axis of the beam-column

γ_x and γ_y shear distortion of the member cross section caused by transverse shear in the x- and y-directions, respectively
θ_x and θ_y bending rotations of the member cross section about the x- and y-axes
$\psi\ (z, t)$ torsional rotation about the shear center S along the z-axis of the member [$=\Psi(z)\sin\omega t$]
κ_{ax}, κ_{bx} and κ_{bx}, κ_{by} stiffness of the rotational restraints at ends A and B about the x- and y-axes, respectively
$\kappa_{a\psi}$ and $\kappa_{b\psi}$ stiffness of the torsional end restraints at ends A and B, respectively (force $\times$ distance/radian)

1. Introduction

The stability and dynamic behavior of beams and beam-columns are of great importance in structural dynamics, aerospace and earthquake engineering. The vibration analysis and seismic response of framed structures modeled as 2D beams and columns have been studied by many researchers and treated extensively in the literature (see Thomson [1], Blevins [2], Berg [3], Paz [4], Clough and Penzien [5], Chopra [6], among others) using different methods. Aristizabal-Ochoa [7] has shown that the classic solutions for the vibration of 2D beams and beam-columns based on the Bernoulli–Euler theory (that neglects the combined effects of shear deflections and rotational inertias along the member) violate the equation of bending moment equilibrium, and consequently violate the principle of conservation of angular momentum. To overcome these deficiencies Aristizabal-Ochoa [8,9] developed a method that determines the buckling loads and natural frequencies of 2D shear beam-columns and shear buildings with generalized end conditions subjected to concentric linear axial load along the member including the effects of end rotations and rotational inertias as well as the P-Delta effects. However, 2D models generally do not take into account the real 3D behavior and the couplings amongst all deflections (shear, torsional and rotational) and the translational, rotational and torsional inertias, as well as the second-order (or P-Delta) effects.

The dynamics of 3D beams and beam-columns have been studied by many researchers. Banerjee et al. [10] studied the warping effects on the natural frequencies of thin-walled beams with open sections. Banerjee [11] analyzed the influence of the axial load on the natural frequencies of a cantilever beam. Li [12] presented the dynamic transfer matrix based on Bernoulli–Euler beam theory including warping effects. Rafezy and Howson [13] developed the dynamic stiffness matrix for a 3D shear beam with asymmetric cross section neglecting the effects of the axial load and bending rotations. More recently, Viola et al. [14] investigated the changes in the magnitude of natural frequencies and modal response introduced by the presence of a crack on an axially loaded uniform Timoshenko beam using the dynamic stiffness matrix. However, studies on the stability and free vibration of 3D beam-columns with generalized end conditions including the combined effects of shear and bending deformations, translational, rotational and torsional inertias as well as P-Delta effects are practically nonexistent. Therefore, there is a real need for a practical approach by which the stability and dynamic characteristics (i.e., buckling loads, natural frequencies and modal shapes) of 3D asymmetrical beam-columns with any end support conditions can be determined directly.

The main objective of this paper is to derive using the "modified" shear equation described by Timoshenko and Gere [15] the characteristic equations for the undamped natural frequencies and the corresponding modes of vibration of an orthotropic singly symmetrical 3D Timoshenko beam-column with generalized support conditions (i.e., with semirigid flexural restraints and lateral bracings as well as lumped masses at both ends) subject to a constant eccentric axial load at both ends. The proposed model is an extension of a 2D shear beam-column model developed by Aristizabal-Ochoa [7] and is more general than any other model available in the literature including that presented by Banerjee [11], since it includes generalized support conditions, orthotropic material properties, the effects of the shear force components induced by the applied axial force as the member bends according to the "modified" shear equation (or Haringx approach), and end masses. All these additional considerations and effects are important in the analysis and design of buildings and beam structures with semirigid connections, particularly when made of composite materials. The effects of the shear force component induced by the applied axial force as the member bends about one of its principal axis and buckling (under both axial tension and compression forces) have been investigated experimentally and analytically by Kelly [16], Roberts [17], and discussed recently by Aristizabal-Ochoa [18]. However, the effects of warping torsion are not included in this study since it would require a much more complex model. To include these effects the model would become extremely complex since it must include not only warping boundary conditions at both ends, but also the three dimensional couplings between "mixed" torsion and biaxial bending caused by the applied loads as explained by Curver [19]. This objective is beyond the scope of this paper. Consequently, the proposed method is not capable of capturing the phenomena of torsional buckling or combined bending–torsional buckling reported by Timoshenko and Gere [20, pp. 225 and 229]. Four examples are included that show the simplicity and versatility of the proposed model and corresponding equations in the shear–bending–torsional free vibration of an orthotropic singly symmetrical 3D beam-columns with generalized support conditions.

2. Structural model

Consider the singly symmetric 3D Timoshenko beam-column shown in Fig. 1 of length span L with closed cross section with the shear center S located a distance x_α from its centroid or mass center C along the axis of symmetry x. It is assumed that the member is prismatic with straight centroidal axis z, subject to a constant axial load P (+ tension, − compression) applied at both ends and along the z-axis, and mass per unit length $\overline{m}$. Two rigid masses of magnitude M_a and M_b are attached to its ends A and B with the corresponding rotational and torsional inertias $J_{ax}, J_{ay}, J_{a\psi}$ and $J_{bx}, J_{by}, J_{b\psi}$ about the x-, y- and z-axes, respectively. The properties of the member include: moments of inertia I_x and I_y about its cross section main centroidal axes x and y; torsional moment of inertia J and torsional shear modulus G_{xy}; cross-section area A and axial modulus E_z; effective shear-areas A_{sx} and A_{sy} with the corresponding shear moduli G_x and G_y; end torsional restraints $\kappa_{a\psi}$ and $\kappa_{b\psi}$; end bending restraints κ_{ax}, κ_{bx} and κ_{ay}, κ_{by} about the local principal x- and y-axes, and end lateral restraints S_{ax}, S_{bx} and S_{ay}, S_{by} along the local principal x- and y-axes, respectively. Note that the end bending restraints κ_{ax}, κ_{bx} and κ_{ay}, κ_{by} as well as the end torsional restraints $\kappa_{a\psi}$ and $\kappa_{b\psi}$ (whose dimensions are in force–distance/radian) vary from zero for perfectly hinged connections to infinity for fully restrained connections (i.e., perfectly clamped conditions). Likewise the end lateral restraints S_{ax}, S_{bx} and S_{ay}, S_{by} (whose dimensions are in force/distance) vary from zero for unbraced end connections to infinity for fully braced end connections.

The elastic axis (assumed to coincide with the z-axis) deforms with translations $u(z, t)$ and $v(z, t)$ in the x- and y-directions, respectively, and with a torsional rotation $\psi(z, t)$ about the z-axis (where t denotes time). Note that for the singly symmetric beam-column of Fig. 1, the translation $u(z, t)$ which takes place in the xz-plane is uncoupled with the torsional rotation $\psi(z, t)$, whereas the translation $v(z, t)$ is coupled with $\psi(z, t)$. Two additional degrees of freedom must be added, these are θ_x and θ_y which represent the rotations of the member cross section caused by the bending moments about the x- and y-axes, respectively. The buckling and free vibration analyses about the x–z and yz-planes of a singly symmetric Timoshenko beam-column are shown in the following sections.

2.1. Buckling and free vibration analyses in the xz-plane

Eqs. (1) and (2) can be obtained applying transverse and bending moment equilibrium when the member deflects in the xz-plane:

$$\frac{\partial H_x}{\partial z} = \overline{m}\frac{\partial^2 u}{\partial t^2}, \tag{1}$$

$$\frac{\partial M_y}{\partial z} = H_x - P\frac{\partial u}{\partial z} - \overline{m}L^2 r_y^2 \frac{\partial^2 \theta_y}{\partial t^2}. \tag{2}$$

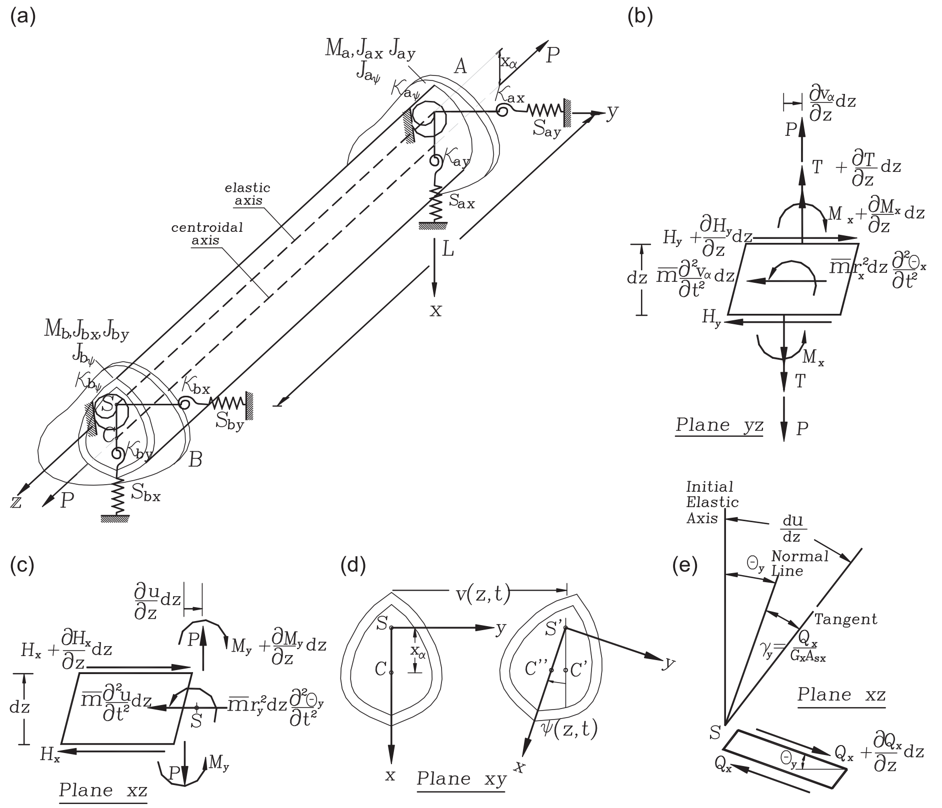

Fig. 1. Structural model: (a) member properties, masses and end connections; (b) forces and moments on the infinitesimal element (*yz*-plane); (c) forces and moments on the infinitesimal element (*xz*-plane); (d) displacements of the closed cross section during the vibration in the *xz*-plane; and (e) bending and shear deformations at a cross section in the *xz*-plane.

According to Haringx's approach (explained by Timoshenko and Gere [15]): $Q_x = H_x - P\theta_y = G_xA_{sx}\gamma_y$ and

$$\gamma_y = \frac{\partial u}{\partial z} - \theta_y, \tag{3}$$

$$H_x = G_xA_{sx}\left(\frac{\partial u}{\partial z} - \theta_y\right) + P\theta_y, \tag{4}$$

$$M_y = -E_zI_y\frac{\partial \theta_y}{\partial z}. \tag{5}$$

Using expressions (3)–(5), equilibrium Eqs. (1) and (2) can be expressed as follows:

$$G_xA_{sx}\left(\frac{\partial^2 u}{\partial z^2} - \frac{\partial \theta_y}{\partial z}\right) + P\frac{\partial \theta_y}{\partial z} - \overline{m}\frac{\partial^2 u}{\partial t^2} = 0, \tag{6}$$

$$E_zI_y\frac{\partial^2 \theta_y}{\partial z^2} + (G_xA_{sx} - P)\left(\frac{\partial u}{\partial z} - \theta_y\right) - \overline{m}L^2r_y^2\frac{\partial^2 \theta_y}{\partial t^2} = 0. \tag{7}$$

The solutions to Eqs. (6) and (7) with P (+ tension, − compression) are assumed to be of the form:

$$u(z,t) = U(z)\sin\omega t, \tag{8}$$

$$\theta_y(z,t) = \Theta_y(z)\sin\omega t. \tag{9}$$

Substituting expressions (8) and (9) into Eqs. (6) and (7):

$$G_xA_{sx}\left(\frac{\partial^2 U}{\partial z^2} - \frac{\partial \Theta_y}{\partial z}\right) + P\frac{\partial \Theta_y}{\partial z} + \overline{m}\omega^2 U = 0, \tag{10}$$

$$E_z I_y \frac{\partial^2 \Theta_y}{\partial z^2} + (G_x A_{sx} - P)\left(\frac{\partial U}{\partial z} - \Theta_y\right) + \overline{m} L^2 r_y^2 \omega^2 \Theta_y = 0. \tag{11}$$

Eqs. (10) and (11) can be reduced to a single differential equation of four-order as follows:

$$\frac{\mathrm{d}^4 U}{\mathrm{d}\xi^4} + (p_u^4 s_u^2 + b_u^2 s_u^2 - p_u^2 + b_u^2 r_y^2)\frac{\mathrm{d}^2 U}{\mathrm{d}\xi^2} + (b_u^2 p_u^2 s_u^2 + b_u^4 s_u^2 r_y^2 - b_u^2)U = 0, \tag{12}$$

where $\xi = z/L$; $b_u^2 = \overline{m}\omega^2 L^4/E_z I_y$; $p_u^2 = PL^2/E_z I_y$ (axial-load parameter); $s_u^2 = E_z I_y / G_x A_{sx} L^2$ (bending-to-shear stiffness parameter); and $r_y^2 = I_y/AL^2$ (slenderness parameter).

The solution to Eq. (12) is of the form U=ce^{mz} which after being substituted into Eq. (12) yields the following auxiliary equation:

$$m^4 + (p_u^4 s_u^2 + b_u^2 s_u^2 - p_u^2 + b_u^2 r_y^2)m^2 + (b_u^2 p_u^2 s_u^2 + b_u^4 s_u^2 r_y^2 - b_u^2) = 0. \tag{13}$$

The solution to Eq. (13) is of the form:

$$m^2 = -\Omega \pm \varepsilon, \tag{14}$$

where

$$\Omega = \frac{(p_u^4 s_u^2 + b_u^2 s_u^2 - p_u^2 + b_u^2 r_y^2)}{2};$$

and

$$\varepsilon = \sqrt{\tfrac{1}{4}(p_u^4 s_u^2 + b_u^2 s_u^2 - p_u^2 + b_u^2 r_y^2)^2 - (b_u^2 p_u^2 s_u^2 + b_u^4 s_u^2 r_y^2 - b_u^2)}.$$

Therefore, the four roots are

$$m = \pm \chi\sqrt{-1} \pm \eta, \tag{15}$$

where $\chi = \sqrt{\varepsilon + \Omega}$; and $\eta = \sqrt{\varepsilon - \Omega}$.

The lateral deflection U can now be expressed as follows:

$$U(\xi) = F_1 \cosh \eta\xi + F_2 \sinh \eta\xi + F_3 \cos \chi\xi + F_4 \sin \chi\xi \tag{16}$$

and the rotation Θ_y of the cross section caused by bending along the member:

$$\Theta_y(\xi) = \frac{\delta}{L}[F_1 \sinh \eta\xi + F_2 \cosh \eta\xi] + \frac{\lambda}{L}[F_3 \sin \chi\xi - F_4 \cos \chi\xi]. \tag{17}$$

Now, applying the following four boundary conditions (i.e., transverse and rotational dynamic equilibrium at the ends) in terms of the nondimensional parameters as the member AB deflects on the xz-plane:

$$\text{At A } \xi = 0: \left(\frac{\mathrm{d}U}{\mathrm{d}\xi}\right)_a + (p_u^2 s_u^2 - 1)\Theta_{ay} - (\overline{S}_{ax} - \overline{M}_a b_u^2 s_u^2)U_a = 0, \tag{18}$$

$$\left(\frac{\mathrm{d}\Theta_y}{\mathrm{d}\xi}\right)_a - (R_{ay} - \overline{J}_{ay} b_u^2)\Theta_{ay} = -p_u^2 \overline{x}_\alpha. \tag{19}$$

$$\text{At B } \xi = 1: \left(\frac{\mathrm{d}U}{\mathrm{d}\xi}\right)_b + (p_u^2 s_u^2 - 1)\Theta_{by} + (\overline{S}_{bx} - \overline{M}_b b_u^2 s_u^2)U_b = 0, \tag{20}$$

$$\left(\frac{\mathrm{d}\Theta_y}{\mathrm{d}\xi}\right)_b + (R_{by} - \overline{J}_{by} b_u^2)\Theta_{by} = -p_u^2 \overline{x}_\alpha. \tag{21}$$

Using expressions (16) and (17) the following expressions can be obtained directly:

$$\frac{\mathrm{d}U}{\mathrm{d}\xi} = F_1 \eta \sinh \eta\xi + F_2 \eta \cosh \eta\xi - F_3 \chi \sin \chi\xi + F_4 \chi \cos \chi\xi;$$

$$\frac{\mathrm{d}\Theta_y}{\mathrm{d}\xi} = \delta\eta[F_1 \cosh \eta\xi + F_2 \sinh \eta\xi] + \lambda\chi[F_3 \cos \chi\xi + F_4 \sin \chi\xi];$$

$$U_a = F_1 + F_3; U_b = F_1 \cosh \eta + F_2 \sinh \eta + F_3 \cos \chi + F_4 \sin \chi;$$

$$\left(\frac{\mathrm{d}U}{\mathrm{d}\xi}\right)_a = \eta F_2 + \chi F_4; \left(\frac{\mathrm{d}U}{\mathrm{d}\xi}\right)_b = \eta(F_1 \sinh \eta + F_2 \cosh \eta) - \chi(F_3 \sin \chi - F_4 \cos \chi);$$

$$\Theta_{ay} = \delta F_2 - \lambda F_4; \Theta_{by} = \delta[F_1 \sinh\eta + F_2 \cosh\eta] + \lambda[F_3 \sin\chi - F_4 \cos\chi];$$

$$\left(\frac{d\Theta_y}{d\xi}\right)_a = \delta\eta F_1 + \lambda\chi F_3; \left(\frac{d\Theta_y}{d\xi}\right)_b = \delta\eta[F_1 \cosh\eta + F_2 \sinh\eta] + \lambda\chi[F_3 \cos\chi + F_4 \sin\chi];$$

where

$$\lambda = \frac{-\chi^2 + b_u^2 s_u^2}{\chi(1 - p_u^2 s_u^2)} \text{and} \delta = \frac{\eta^2 + b_u^2 s_u^2}{\eta(1 - p_u^2 s_u^2)}.$$

Characteristic equation. Eqs. (18)–(21) can be expressed in matrix form as follows:

$$\begin{bmatrix} c_{11} & c_{12} & c_{13} & c_{14} \\ c_{21} & c_{22} & c_{23} & c_{24} \\ c_{31} & c_{32} & c_{33} & c_{34} \\ c_{41} & c_{42} & c_{43} & c_{44} \end{bmatrix} \begin{Bmatrix} F_1 \\ F_2 \\ F_3 \\ F_4 \end{Bmatrix} = \begin{Bmatrix} 0 \\ -p_u^2 \overline{x}_\alpha \\ 0 \\ -p_u^2 \overline{x}_\alpha \end{Bmatrix}, \tag{22}$$

where

$$\overline{x}_\alpha = x_\alpha / L; \quad c_{11} = c_{13} = -(\overline{S}_{ax} - b_u^2 s_u^2 \overline{M}_a); \quad c_{12} = \eta + (p_u^2 s_u^2 - 1)\delta;$$

$$c_{14} = \chi - (p_u^2 s_u^2 - 1)\lambda; \quad c_{21} = \delta\eta; \quad c_{22} = -(R_{ay} - b_u^2 \overline{J}_{ay})\delta; \quad c_{23} = \lambda\chi; c_{24} = (R_{ay} - b_u^2 \overline{J}_{ay})\lambda;$$

$$c_{31} = \lfloor \eta + (p_u^2 s_u^2 - 1)\delta \rfloor \sinh\eta + (\overline{S}_{bx} - b_u^2 s_u^2 \overline{M}_b)\cosh\eta; \quad c_{32} = \lfloor \eta + (p_u^2 s_u^2 - 1)\delta \rfloor \cosh\eta + (\overline{S}_{bx} - b_u^2 s_u^2 \overline{M}_b)\sinh\eta;$$

$$c_{33} = \lfloor -\chi + (p_u^2 s_u^2 - 1)\lambda \rfloor \sin\chi + (\overline{S}_{bx} - b_u^2 s_u^2 \overline{M}_b)\cos\chi; \quad c_{34} = \lfloor \chi - (p_u^2 s_u^2 - 1)\lambda \rfloor \cos\chi + (\overline{S}_{bx} - b_u^2 s_u^2 \overline{M}_b)\sin\chi;$$

$$c_{41} = \delta\eta \cosh\eta + (R_{by} - b_u^2 \overline{J}_{by})\delta \sinh\eta; \quad c_{42} = \delta\eta \sinh\eta + (R_{by} - b_u^2 \overline{J}_{by})\delta \cosh\eta;$$

$$c_{43} = \lfloor \lambda\chi \cos\chi + (R_{by} - b_u^2 \overline{J}_{by})\lambda \sin\chi \rfloor \quad \text{and} \quad c_{44} = \lfloor \lambda\chi \sin\chi - (R_{by} - b_u^2 \overline{J}_{by})\lambda \cos\chi \rfloor.$$

Eq. (22) represents the dynamic stability of a singly symmetric Timoshenko beam-column with generalized end conditions when it bends in the *xz*-plane only.

2.2. Buckling and free vibration analyses in the yz-plane (shear–bending–torsional coupling)

Knowing that the relationship between the lateral deflection of the centroid and the shear center is

$$v_\alpha = v - x_\alpha \psi; \tag{23}$$

$$\textit{Transverse Equilibrium}: \frac{\partial H_y}{\partial z} = \overline{m}\frac{\partial^2 v_\alpha}{\partial t^2} = \overline{m}\left(\frac{\partial^2 v}{\partial t^2} - x_\alpha \frac{\partial^2 \psi}{\partial t^2}\right); \tag{24}$$

$$\textit{Bending Moment Equilibrium}: \frac{\partial M_x}{\partial z} = H_y - P\left(\frac{\partial v}{\partial z} - x_\alpha \frac{\partial \psi}{\partial z}\right) - \overline{m}L^2 r_x^2 \frac{\partial^2 \theta_x}{\partial t^2}; \tag{25}$$

$$\textit{Torsional Moment Equilibrium}: \frac{\partial T}{\partial z} = I_\alpha \frac{\partial^2 \psi}{\partial t^2} - \overline{m} x_\alpha \frac{\partial^2 v}{\partial t^2}; \tag{26}$$

where $I_\alpha = (\overline{m}/A)(I_x + I_y) + \overline{m} x_\alpha^2$.

Using Haringx's approach (explained by Timoshenko and Gere [15]): $Q_y = H_y - P\theta_x = G_y A_{sy} \gamma_x$ and

$$\gamma_x = \frac{\partial v}{\partial z} - \theta_x, \tag{27}$$

$$H_y = G_y A_{sy}\left(\frac{\partial v}{\partial z} - \theta_x\right) + P\theta_x. \tag{28}$$

Knowing that

$$T = G_{xy} J \frac{\partial \psi}{\partial z} + P\frac{I_\alpha}{\overline{m}}\frac{\partial \psi}{\partial z} - P x_\alpha \frac{\partial v}{\partial z}, \tag{29}$$

and

$$M_x = -E_z I_x \frac{\partial \theta_x}{\partial z}. \tag{30}$$

Substituting expressions (27)–(30) into Eqs. (24)–(26):

$$G_yA_{sy}\left(\frac{\partial^2 v}{\partial z^2}-\frac{\partial\theta_x}{\partial z}\right)+P\frac{\partial\theta_x}{\partial z}-\overline{m}\left(\frac{\partial^2 v}{\partial t^2}-x_\alpha\frac{\partial^2\psi}{\partial t^2}\right)=0, \tag{31}$$

$$E_zI_x\frac{\partial^2\theta_x}{\partial z^2}+(G_yA_{sy}-P)\left(\frac{\partial v}{\partial z}-\theta_x\right)+Px_\alpha\frac{\partial\psi}{\partial z}-\overline{m}L^2r_x^2\frac{\partial^2\theta_x}{\partial t^2}=0, \tag{32}$$

$$G_{xy}J\frac{\partial^2\psi}{\partial z^2}+P\left(\frac{I_\alpha}{\overline{\overline{m}}}\frac{\partial^2\psi}{\partial z^2}-x_\alpha\frac{\partial^2 v}{\partial z^2}\right)-I_\alpha\frac{\partial^2\psi}{\partial t^2}+\overline{m}x_\alpha\frac{\partial^2 v}{\partial t^2}=0. \tag{33}$$

Also knowing that $\overline{m}=\rho A$ and $Lr_x=\sqrt{I_x/A}$, Eqs. (31)–(33) become

$$G_yA_{sy}(v''-\theta_x')+P\theta_x'-\overline{m}(\ddot{v}-x_\alpha\ddot{\psi})=0, \tag{34}$$

$$E_zI_x\theta_x''+(G_yA_{sy}-P)(v'-\theta_x)+Px_\alpha\psi'-\rho I_x\ddot{\theta}_x=0, \tag{35}$$

$$G_{xy}J\psi''+P\left(\frac{I_\alpha}{\overline{\overline{m}}}\psi''-x_\alpha v''\right)-I_\alpha\ddot{\psi}+\overline{m}x_\alpha\ddot{v}=0. \tag{36}$$

The solutions to Eqs. (34)–(37) are of the form

$$v(z,t)=V(z)\sin\omega t, \tag{37}$$

$$\theta_x(z,t)=\Theta_x(z)\sin\omega t, \tag{38}$$

$$\psi(z,t)=\Psi(z)\sin\omega t. \tag{39}$$

Substituting expressions (37)–(39) into Eqs. (34)–(36):

$$G_yA_{sy}(V''-\Theta_x')+P\Theta_x'+\overline{m}\omega^2V-\overline{m}\omega^2x_\alpha\Psi=0, \tag{34a}$$

$$E_zI_x\Theta_x''+(G_yA_{sy}-P)(V'-\Theta_x)+Px_\alpha\Psi'+\rho I_x\omega^2\Theta_x=0, \tag{35a}$$

$$G_{xy}J\Psi''+P\left(\frac{I_\alpha}{\overline{\overline{m}}}\Psi''-x_\alpha V''\right)+I_\alpha\omega^2\Psi-\overline{m}\omega^2x_\alpha V=0. \tag{36a}$$

Introducing the nondimensional length $\xi=z/L$, and differential operator $D=\mathrm{d}/\mathrm{d}\xi$ and applying the chain's rule:

$$G_yA_{sy}(V''-L\Theta_x')+PL\Theta_x'+\overline{m}\omega^2L^2V-\overline{m}\omega^2x_\alpha L^2\Psi=0, \tag{34b}$$

$$E_zI_x\Theta_x''+(G_yA_{sy}-P)(LV'-L^2\Theta_x)+Px_\alpha L\Psi'+\rho I_x\omega^2L^2\Theta_x=0, \tag{35b}$$

$$G_{xy}J\Psi''+P\left(\frac{I_\alpha}{\overline{\overline{m}}}\Psi''-x_\alpha V''\right)+I_\alpha\omega^2L^2\Psi-\overline{m}\omega^2x_\alpha L^2V=0. \tag{36b}$$

Eqs. (34b)–(36b) expressed in matrix form become

$$\begin{bmatrix} G_yA_{sy}D^2+\overline{m}\omega^2L^2 & (P-G_yA_{sy})LD & -\overline{m}\omega^2x_\alpha L^2 \\ (G_yA_{sy}-P)LD & E_zI_xD^2+(P-G_yA_{sy})L^2+\rho I_x\omega^2L^2 & Px_\alpha LD \\ -Px_\alpha D^2-\overline{m}\omega^2x_\alpha L^2 & 0 & G_{xy}JD^2+P\frac{I_\alpha}{\overline{\overline{m}}}D^2+I_\alpha\omega^2L^2 \end{bmatrix}\begin{Bmatrix} V \\ \Theta_x \\ \Psi \end{Bmatrix}=0 \tag{37a}$$

Using Gauss elimination and expanding the determinant:

$$(D^6+\overline{a}D^4-\overline{b}D^2-\overline{c})T=0 \quad \text{with } T=V,\ \Theta_x \text{ or } \Psi, \tag{38a}$$

where

$$\overline{a}=b^2r_x^2+\frac{a^2b^2(1+c^2p^2s^2)-a^2c^2p^4-b^2(p^2-b^2s^2)+p^4s^2(b^2+a^2c^2p^2)}{b^2+a^2p^2};$$

$$\overline{b}=\frac{b^4(1-b^2s^2r_x^2)-a^2b^4c^2s^2(1+p^2r_x^2)+a^2b^2(2c^2p^2-b^2r_x^2)-b^2p^2s^2(b^2+2a^2c^2p^2)}{b^2+a^2p^2};$$

and

$$\overline{c} = \frac{a^2 b^4 c^2 (1 - b^2 r_x^2 s^2 - p^2 s^2)}{b^2 + a^2 p^2}.$$

The stability and free vibration analyses of the singly symmetric 3D orthotropic Timoshenko beam-column of Fig. 1 depend on the following 34 variables: E_z, G_x, G_y, G_{xy}, A, A_{sx}, A_{sy}, I_x, I_y, I_α, J, L, x_α, P, $\overline{m}$, ω, κ_{ax}, κ_{ay}, $\kappa_{a\psi}$, κ_{bx}, κ_{by}, $\kappa_{b\psi}$, S_{ax}, S_{ay}, S_{bx}, S_{by}, M_a, M_b, J_{ax}, J_{ay}, $J_{a\psi}$, J_{bx}, J_{by} and $J_{b\psi}$. However, these variables can be grouped into 28 dimensionless parameters and indices as follows: $a^2 = I_\alpha \omega^2 L^2 / G_{xy} J$, $b_u^2 = \overline{m}\omega^2 L^4 / E_z I_y$, $b^2 = \overline{m}\omega^2 L^4 / E_z I_x$ (frequency parameters); $c^2 = 1 - \overline{m} x_\alpha^2 / I_\alpha$ (axial-load eccentricity parameter); $p_u^2 = PL^2/E_z I_y$, $p^2 = PL^2/E_z I_x$ (axial-load parameters); $s_u^2 = E_z I_y / G_x A_{sx} L^2$, $s^2 = E_z I_x / G_y A_{sy} L^2$ (bending-to-shear stiffness parameters); $r_x^2 = I_x/AL^2$, $r_y^2 = I_y/AL^2$ (slenderness parameter); $R_{ax} = \kappa_{ax}/(E_z I_x/L)$, $R_{ay} = \kappa_{ay}/(E_z I_y/L)$, $R_{bx} = \kappa_{bx}/(E_z I_x/L)$, $R_{by} = \kappa_{by}/(E_z I_y/L)$ (bending indices at ends A and B, respectively); $\overline{S}_{ax} = S_{ax}/(G_x A_{sx}/L)$, $\overline{S}_{ay} = S_{ay}/(G_y A_{sy}/L)$ and $\overline{S}_{bx} = S_{bx}/(G_x A_{sx}/L)$, $\overline{S}_{by} = S_{by}/(G_y A_{sy}/L)$ (lateral bracing indices at ends A and B, respectively); $\overline{M}_a = M_a/\overline{m}L$ and $\overline{M}_b = M_b/\overline{m}L$ (mass indices at ends A and B, respectively); $\bar{J}_{ax} = J_{ax}/\overline{m}L^3$, $\bar{J}_{ay} = J_{ay}/\overline{m}L^3$, $\bar{J}_{bx} = J_{bx}/\overline{m}L^3$, $\bar{J}_{by} = J_{by}/\overline{m}L^3$ (rotational-mass indices at ends A and B, respectively); $\bar{J}_{a\psi} = J_{a\psi}/I_\alpha L$, $\bar{J}_{b\psi} = J_{b\psi}/I_\alpha L$ (torsional-mass indices at ends A and B, respectively); and $\overline{\kappa}_{a\psi} = \kappa_{a\psi}/(G_{xy}J/L)$ and $\overline{\kappa}_{b\psi} = \kappa_{b\psi}/(G_{xy}J/L)$ (torsional indices at A and B, respectively).

Solutions to Eq. (38) are taken from (http://mathworld.wolfram.com/search/) as follows:

$$\alpha = \left[2\sqrt{\frac{q}{3}}\cos\left(\frac{\phi}{3}\right) - \frac{\overline{a}}{3}\right]^{1/2}; \quad \beta = \left[2\sqrt{\frac{q}{3}}\cos\left(\frac{\pi-\phi}{3}\right) + \frac{\overline{a}}{3}\right]^{1/2}; \quad \gamma = \left[2\sqrt{\frac{q}{3}}\cos\left(\frac{\pi+\phi}{3}\right) + \frac{\overline{a}}{3}\right]^{1/2},$$

where

$$q = \overline{b} + \frac{1}{3}(\overline{a})^2 \quad \text{and} \quad \phi = \cos^{-1}\frac{(27\overline{c} - 9\overline{a}\overline{b} - 2\overline{a}^3)}{2(\overline{a}^2 + 3\overline{b})^{3/2}}.$$

The displacement $V(\xi)$, bending rotation $\Theta_x(\xi)$, and torsional rotation $\Psi(\xi)$ are expressed as follows:

$$V(\xi) = A_1 \cosh\alpha\xi + A_2 \sinh\alpha\xi + A_3 \cos\beta\xi + A_4 \sin\beta\xi + A_5 \cos\gamma\xi + A_6 \sin\gamma\xi; \tag{39a}$$

$$\Theta_x(\xi) = B_1 \sinh\alpha\xi + B_2 \cosh\alpha\xi + B_3 \sin\beta\xi + B_4 \cos\beta\xi + B_5 \sin\gamma\xi + B_6 \cos\gamma\xi; \tag{40}$$

$$\Psi(\xi) = C_1 \cosh\alpha\xi + C_2 \sinh\alpha\xi + C_3 \cos\beta\xi + C_4 \sin\beta\xi + C_5 \cos\gamma\xi + C_6\, sin\,\gamma\xi. \tag{41}$$

From Eq. (34a):

$$\Psi = \frac{G_y A_{sy}(V'' - \Theta_x') + P\Theta_x' + \overline{m}\omega^2 V}{\overline{m}\omega^2 x_\alpha}. \tag{42}$$

Substituting expressions (39), (40) and (42) into Eq. (35a), coefficients B_1–B_6 are obtained in terms of coefficients A_1–A_6 as follows:

$$B_1 = A_1\overline{\alpha}/L; \quad B_2 = A_2\overline{\alpha}/L; \quad B_3 = -A_3\overline{\beta}/L; \quad B_4 = A_4\overline{\beta}/L; \quad B_5 = -A_5\overline{\gamma}/L; \quad \text{and} \quad B_6 = A_6\overline{\gamma}/L;$$

where

$$\overline{\alpha} = \frac{\alpha(1 + \alpha^2 b^{-2} p^2)}{1 - b^2 s^2 r_x^2 - \alpha^2 s^2 - p^2 s^2 (1 + \alpha^2 b^{-2} p^2) + \alpha^2 b^{-2} p^2};$$

$$\overline{\beta} = \frac{\beta(1 - \beta^2 b^{-2} p^2)}{1 - b^2 s^2 r_x^2 + \beta^2 s^2 - p^2 s^2 (1 - \beta^2 b^{-2} p^2) - \beta^2 b^{-2} p^2};$$

$$\overline{\gamma} = \frac{\gamma(1 - \gamma^2 b^{-2} p^2)}{1 - b^2 s^2 r_x^2 + \gamma^2 s^2 - p^2 s^2 (1 - \gamma^2 b^{-2} p^2) - \gamma^2 b^{-2} p^2}.$$

Likewise, substituting expressions (39), (40) and (42) into Eq. (36a), coefficients C_1–C_6 are obtained in terms of coefficients A_1–A_6 as follows:

$$C_1 = A_1 k_\alpha / x_\alpha; \quad C_2 = A_2 k_\alpha / x_\alpha; \quad C_3 = A_3 k_\beta / x_\alpha;$$

$$C_4 = A_4 k_\beta / x_\alpha; \quad C_5 = A_5 k_\gamma / x_\alpha; \quad C_6 = A_6 k_\gamma / x_\alpha,$$

where

$$k_\alpha = \frac{a^2(b^2 + p^2\alpha^2)(1 - c^2)}{a^2(b^2 + p^2\alpha^2) + b^2\alpha^2}; \quad k_\beta = \frac{a^2(b^2 - p^2\beta^2)(1 - c^2)}{a^2(b^2 - p^2\beta^2) - b^2\beta^2}; \quad k_\gamma = \frac{a^2(b^2 - p^2\gamma^2)(1 - c^2)}{a^2(b^2 - p^2\gamma^2) - b^2\gamma^2};$$

$$\frac{dV}{d\xi} = A_1\alpha\sinh\alpha\xi + A_2\alpha\cosh\alpha\xi - A_3\beta\sin\beta\xi + A_4\beta\cos\beta\xi - A_5\gamma\sin\gamma\xi + A_6\gamma\cos\gamma\xi;$$

$$\frac{d\Theta_x}{d\xi} = \frac{1}{L}[\alpha\overline{\alpha}(A_1\cosh\alpha\xi + A_2\sinh\alpha\xi) - \beta\overline{\beta}(A_3\cos\beta\xi + A_4\sin\beta\xi) - \gamma\overline{\gamma}(A_5\cos\gamma\xi + A_6\sin\gamma\xi)];$$

$$\frac{d\Psi}{d\xi} = \frac{k_\alpha}{x_\alpha}\alpha(A_1\sinh\alpha\xi + A_2\cosh\alpha\xi) - \frac{k_\beta}{x_\alpha}\beta(A_3\sin\beta\xi - A_4\cos\beta\xi) - \frac{k_\gamma}{x_\alpha}\gamma(A_5\sin\gamma\xi - A_6\cos\gamma\xi).$$

From Eq. (28):

$$H_y(\xi) = \left[\frac{dV}{d\xi} + (p^2s^2-1)L\Theta_x\right]\frac{G_yA_{sy}}{L}$$

or

$$H_y(\xi) = [g_\alpha(A_1\sinh\alpha\xi + A_2\cosh\alpha\xi) - g_\beta(A_3\sin\beta\xi - A_4\cos\beta\xi) - g_\gamma(A_5\sin\gamma\xi - A_6\cos\gamma\xi)]\frac{G_yA_{sy}}{L}. \tag{43}$$

From Eq. (29):

$$T(\xi) = \left[\left(1+\frac{a^2p^2}{b^2}\right)\frac{d\Psi}{d\xi} - \frac{a^2p^2(1-c^2)}{x_\alpha b^2}\frac{dV}{d\xi}\right]\frac{G_{xy}J}{L}$$

or

$$T(\xi) = \left[\frac{\alpha e_\alpha}{x_\alpha}(A_1\sinh\alpha\xi + A_2\cosh\alpha\xi) - \frac{\beta e_\beta}{x_\alpha}(A_3\sin\beta\xi - A_4\cos\beta\xi) - \frac{\gamma e_\gamma}{x_\alpha}(A_5\sin\gamma\xi - A_6\cos\gamma\xi)\right]\frac{G_{xy}J}{L}. \tag{44}$$

From Eq. (30):

$$M_x(\xi) = -\frac{E_zI_x}{L}\frac{d\Theta_x}{d\xi}$$

or

$$M_x(\xi) = -[\alpha\overline{\alpha}(A_1\cosh\alpha\xi + A_2\sinh\alpha\xi) - \beta\overline{\beta}(A_3\cos\beta\xi + A_4\sin\beta\xi) - \gamma\overline{\gamma}(A_5\cos\gamma\xi + A_6\sin\gamma\xi)]\frac{E_zI_x}{L^2}, \tag{45}$$

where $g_\alpha = \alpha + (p^2s^2-1)\overline{\alpha}$; $g_\beta = \beta + (p^2s^2-1)\overline{\beta}$; $g_\gamma = \gamma + (p^2s^2-1)\overline{\gamma}$;

$$e_\alpha = \left(1+\frac{a^2p^2}{b^2}\right)k_\alpha - \frac{a^2p^2(1-c^2)}{b^2};\quad e_\beta = \left(1+\frac{a^2p^2}{b^2}\right)k_\beta - \frac{a^2p^2(1-c^2)}{b^2};\quad \text{and}\quad e_\gamma = \left(1+\frac{a^2p^2}{b^2}\right)k_\gamma - \frac{a^2p^2(1-c^2)}{b^2}.$$

Now, applying the boundary conditions when the member bends in the yz-plane and twists about the z-axis simultaneously, the following expressions for the shear forces, bending moments, and torsional moments at the ends A and B can be obtained:

$$\text{At A } (\xi = 0):\quad H_A = (S_{ay} - \omega^2 M_a)V_a; \tag{46a}$$

$$M_A = (-\kappa_{ax} + \omega^2 J_{ax})\Theta_{ax}; \tag{47a}$$

$$T_A = (\kappa_{a\psi} - \omega^2 J_{a\psi})\Psi_a. \tag{48a}$$

$$\text{At B } (\xi = 1): H_B = (-S_{by} + \omega^2 M_b)V_b; \tag{49a}$$

$$M_B = (\kappa_{bx} - \omega^2 J_{bx})\Theta_{bx}; \tag{50a}$$

$$T_B = (-\kappa_{b\psi} + \omega^2 J_{b\psi})\Psi_b. \tag{51a}$$

Eqs. (46a)–(51a) can be expressed terms of the nondimensional parameters as follows:

$$\frac{G_yA_{sy}}{L}\left\{\left(\frac{dV}{d\xi}\right)_a + (p^2s^2L - L)\Theta_{ax} - (\overline{S}_{ay} - \overline{M}_a b^2 s^2)V_a\right\} = 0; \tag{46b}$$

$$\frac{E_zI_x}{L}\left\{\left(\frac{d\Theta_x}{d\xi}\right)_a - (R_{ax} - \bar{J}_{ax}b^2)\Theta_{ax}\right\} = 0; \tag{47b}$$

$$\frac{G_{xy}J}{L}\left\{\left(1+\frac{a^2p^2}{b^2}\right)\left(\frac{\mathrm{d}\Psi}{\mathrm{d}\xi}\right)_a-\frac{a^2p^2(1-c^2)}{x_\alpha b^2}\left(\frac{\mathrm{d}V}{\mathrm{d}\xi}\right)_a-(\overline{\kappa}_{a\psi}-\bar{J}_{a\psi}a^2)\Psi_a\right\}=0; \tag{48b}$$

$$\frac{G_yA_{sy}}{L}\left\{\left(\frac{\mathrm{d}V}{\mathrm{d}\xi}\right)_b+(p^2s^2L-L)\Theta_{bx}+(\overline{S}_{by}-\overline{M}_bb^2s^2)V_b\right\}=0; \tag{49b}$$

$$\frac{E_zI_x}{L}\left\{\left(\frac{\mathrm{d}\Theta_x}{\mathrm{d}\xi}\right)_b+(R_{bx}-\bar{J}_{bx}b^2)\Theta_{bx}\right\}=0; \tag{50b}$$

$$\frac{G_{xy}J}{L}\left\{\left(1+\frac{a^2p^2}{b^2}\right)\left(\frac{\mathrm{d}\Psi}{\mathrm{d}\xi}\right)_b-\frac{a^2p^2(1-c^2)}{x_\alpha b^2}\left(\frac{\mathrm{d}V}{\mathrm{d}\xi}\right)_b+(\overline{\kappa}_{b\psi}-\bar{J}_{b\psi}a^2)\Psi_b\right\}=0. \tag{51b}$$

Characteristic equation. Knowing that

$$V_a=A_1+A_3+A_5;V_b=A_1\cosh\alpha+A_2\sinh\alpha+A_3\cos\beta+A_4\sin\beta+A_5\cos\gamma+A_6\sin\gamma;$$

$$\left(\frac{\mathrm{d}V}{\mathrm{d}\xi}\right)_a=A_2\alpha+A_4\beta+A_6\gamma;$$

$$\left(\frac{\mathrm{d}V}{\mathrm{d}\xi}\right)_b=\alpha(A_1\sinh\alpha+A_2\cosh\alpha)-\beta(A_3\sin\beta-A_4\cos\beta)-\gamma(A_5\sin\gamma-A_6\cos\gamma);$$

$$\Theta_{ax}=\frac{1}{L}(\overline{\alpha}A_2+\overline{\beta}A_4+\overline{\gamma}A_6);$$

$$\Theta_{bx}=\frac{1}{L}[\overline{\alpha}(A_1\sinh\alpha+A_2\cosh\alpha)-\overline{\beta}(A_3\sin\beta-A_4\cos\beta)-\overline{\gamma}(A_5\sin\gamma-A_6\cos\gamma)];$$

$$\left(\frac{\mathrm{d}\Theta_x}{\mathrm{d}\xi}\right)_a=\frac{1}{L}(A_1\alpha\overline{\alpha}-A_3\beta\overline{\beta}-A_5\gamma\overline{\gamma});$$

$$\left(\frac{\mathrm{d}\Theta_x}{\mathrm{d}\xi}\right)_b=\frac{1}{L}[\alpha\overline{\alpha}(A_1\cosh\alpha+A_2\sinh\alpha)-\beta\overline{\beta}(A_3\cos\beta+A_4\sin\beta)-\gamma\overline{\gamma}(A_5\cos\gamma+A_6\,sin\,\gamma)];$$

$$\Psi_a=A_1\frac{k_\alpha}{x_\alpha}+A_3\frac{k_\beta}{x_\alpha}+A_5\frac{k_\gamma}{x_\alpha};$$

$$\Psi_b=\frac{k_\alpha}{x_\alpha}(A_1\mathrm{cosh}\alpha+A_2\mathrm{sinh}\alpha)+\frac{k_\beta}{x_\alpha}(A_3\mathrm{cos}\beta+A_4\mathrm{sin}\beta)+\frac{k_\gamma}{x_\alpha}(A_5\mathrm{cos}\gamma+A_6\mathrm{sin}\gamma);$$

$$\left(\frac{\mathrm{d}\Psi}{\mathrm{d}\xi}\right)_a=A_2\frac{k_\alpha}{x_\alpha}\alpha+A_4\frac{k_\beta}{x_\alpha}\beta+A_6\frac{k_\gamma}{x_\alpha}\gamma;$$

$$\left(\frac{\mathrm{d}\Psi}{\mathrm{d}\xi}\right)_b=\frac{k_\alpha}{x_\alpha}\alpha(A_1\mathrm{sinh}\alpha+A_2\mathrm{cosh}\alpha)-\frac{k_\beta}{x_\alpha}\beta(A_3\mathrm{sin}\beta-A_4\mathrm{cos}\beta)-\frac{k_\gamma}{x_\alpha}\gamma(A_5\mathrm{sin}\gamma-A_6\mathrm{cos}\gamma).$$

Substituting these expressions into Eqs. (46b)–(51b), the 6×6 matrix Eq. (52) can be obtained

$$\begin{bmatrix} a_{11} & a_{12} & a_{13} & a_{14} & a_{15} & a_{16}\\ a_{21} & a_{22} & a_{23} & a_{24} & a_{25} & a_{26}\\ a_{31} & a_{32} & a_{33} & a_{34} & a_{35} & a_{36}\\ a_{41} & a_{42} & a_{43} & a_{44} & a_{45} & a_{46}\\ a_{51} & a_{52} & a_{53} & a_{54} & a_{55} & a_{56}\\ a_{61} & a_{62} & a_{63} & a_{64} & a_{65} & a_{66}\end{bmatrix}\begin{Bmatrix} A_1\\ A_2\\ A_3\\ A_4\\ A_5\\ A_6\end{Bmatrix}=0, \tag{52}$$

where

$$a_{11}=a_{13}=a_{15}=-(\overline{S}_{ay}-\overline{M}_ab^2s^2);\quad a_{12}=(p^2s^2-1)\overline{\alpha}+\alpha;\quad a_{14}=(p^2s^2-1)\overline{\beta}+\beta;$$

$$a_{16}=(p^2s^2-1)\overline{\gamma}+\gamma;\quad a_{21}=\alpha\overline{\alpha};\quad a_{22}=-(R_{ax}-\bar{J}_{ax}b^2)\overline{\alpha};\quad a_{23}=-\beta\overline{\beta};$$

$$a_{24}=-(R_{ax}-\bar{J}_{ax}b^2)\overline{\beta};\quad a_{25}=-\gamma\overline{\gamma};\quad a_{26}=-(R_{ax}-\bar{J}_{ax}b^2)\overline{\gamma};$$

$$a_{31} = -(\overline{\kappa}_{a\psi} - \bar{J}_{a\psi}a^2)\frac{k_\alpha}{x_\alpha}; \quad a_{32} = \left[\left(1+\frac{a^2p^2}{b^2}\right)\frac{k_\alpha}{x_\alpha} - \frac{a^2p^2(1-c^2)}{x_\alpha b^2}\right]\alpha;$$

$$a_{33} = -(\overline{\kappa}_{a\psi} - \bar{J}_{a\psi}a^2)\frac{k_\beta}{x_\alpha}; \quad a_{34} = \left[\left(1+\frac{a^2p^2}{b^2}\right)\frac{k_\beta}{x_\alpha} - \frac{a^2p^2(1-c^2)}{x_\alpha b^2}\right]\beta;$$

$$a_{35} = -(\overline{\kappa}_{a\psi} - \bar{J}_{a\psi}a^2)\frac{k_\gamma}{x_\alpha}; \quad a_{36} = \left[\left(1+\frac{a^2p^2}{b^2}\right)\frac{k_\gamma}{x_\alpha} - \frac{a^2p^2(1-c^2)}{x_\alpha b^2}\right]\gamma;$$

$$a_{41} = \lfloor\alpha + (p^2s^2-1)\overline{\alpha}\rfloor\sinh\alpha + (\overline{S}_{by} - \overline{M}_b b^2 s^2)\cosh\alpha;$$

$$a_{42} = \lfloor\alpha + (p^2s^2-1)\overline{\alpha}\rfloor\cosh\alpha + (\overline{S}_{by} - \overline{M}_b b^2 s^2)\sinh\alpha;$$

$$a_{43} = -\lfloor\beta + (p^2s^2-1)\overline{\beta}\rfloor\sin\beta + (\overline{S}_{by} - \overline{M}_b b^2 s^2)\cos\beta;$$

$$a_{44} = \lfloor\beta + (p^2s^2-1)\overline{\beta}\rfloor\cos\beta + (\overline{S}_{by} - \overline{M}_b b^2 s^2)\sin\beta;$$

$$a_{45} = -\lfloor\gamma + (p^2s^2-1)\overline{\gamma}\rfloor\sin\gamma + (\overline{S}_{by} - \overline{M}_b b^2 s^2)\cos\gamma;$$

$$a_{46} = \lfloor\gamma + (p^2s^2-1)\overline{\gamma}\rfloor\cos\gamma + (\overline{S}_{by} - \overline{M}_b b^2 s^2)\sin\gamma;$$

$$a_{51} = \lfloor\alpha\cosh\alpha + (R_{bx} - \bar{J}_{bx}b^2)\sinh\alpha\rfloor\overline{\alpha}; \quad a_{52} = \lfloor\alpha\sinh\alpha + (R_{bx} - \bar{J}_{bx}b^2)\cosh\alpha\rfloor\overline{\alpha};$$

$$a_{53} = -\lfloor\beta\cos\beta + (R_{bx} - \bar{J}_{bx}b^2)\sin\beta\rfloor\overline{\beta}; \quad a_{54} = -\lfloor\beta\sin\beta - (R_{bx} - \bar{J}_{bx}b^2)\cos\beta\rfloor\overline{\beta};$$

$$a_{55} = -\lfloor\gamma\cos\gamma + (R_{bx} - \bar{J}_{bx}b^2)\sin\gamma\rfloor\overline{\gamma}; \quad a_{56} = -\lfloor\gamma\sin\gamma - (R_{bx} - \bar{J}_{bx}b^2)\cos\gamma\rfloor\overline{\gamma};$$

$$a_{61} = \left[\left(1+\frac{a^2p^2}{b^2}\right)\frac{k_\alpha}{x_\alpha} - \frac{a^2p^2(1-c^2)}{x_\alpha b^2}\right]\alpha\sinh\alpha + (\overline{\kappa}_{b\psi} - \bar{J}_{b\psi}a^2)\frac{k_\alpha}{x_\alpha}\cosh\alpha;$$

$$a_{62} = \left[\left(1+\frac{a^2p^2}{b^2}\right)\frac{k_\alpha}{x_\alpha} - \frac{a^2p^2(1-c^2)}{x_\alpha b^2}\right]\alpha\cosh\alpha + (\overline{\kappa}_{b\psi} - \bar{J}_{b\psi}a^2)\frac{k_\alpha}{x_\alpha}\sinh\alpha;$$

$$a_{63} = -\left[\left(1+\frac{a^2p^2}{b^2}\right)\frac{k_\beta}{x_\alpha} - \frac{a^2p^2(1-c^2)}{x_\alpha b^2}\right]\beta\sin\beta + (\overline{\kappa}_{b\psi} - \bar{J}_{b\psi}a^2)\frac{k_\beta}{x_\alpha}\cos\beta;$$

$$a_{64} = \left[\left(1+\frac{a^2p^2}{b^2}\right)\frac{k_\beta}{x_\alpha} - \frac{a^2p^2(1-c^2)}{x_\alpha b^2}\right]\beta\cos\beta + (\overline{\kappa}_{b\psi} - \bar{J}_{b\psi}a^2)\frac{k_\beta}{x_\alpha}\sin\beta;$$

$$a_{65} = -\left[\left(1+\frac{a^2p^2}{b^2}\right)\frac{k_\gamma}{x_\alpha} - \frac{a^2p^2(1-c^2)}{x_\alpha b^2}\right]\gamma\sin\gamma + (\overline{\kappa}_{b\psi} - \bar{J}_{b\psi}a^2)\frac{k_\gamma}{x_\alpha}\cos\gamma;$$

$$a_{66} = \left[\left(1+\frac{a^2p^2}{b^2}\right)\frac{k_\gamma}{x_\alpha} - \frac{a^2p^2(1-c^2)}{x_\alpha b^2}\right]\gamma\cos\gamma + (\overline{\kappa}_{b\psi} - \bar{J}_{b\psi}a^2)\frac{k_\gamma}{x_\alpha}\sin\gamma.$$

Eq. (52) represents the free vibration eigen-value problem of the orthotropic singly symmetric 3D Timoshenko beam-column shown in Fig. 1 when it bends in the yz-plane and twists about the z-axis simultaneously.

3. Methodology to extract frequencies and modes of vibration from Eqs. (22) and (52)

For the free vibration analyses of an orthotropic singly symmetric 3D Timoshenko beam-column with generalized boundary conditions (shown in Fig. 1) the following steps are suggested:

(1) Enter the values of: E_z, G_x, G_y, G_{xy}, A, A_{sx}, A_{sy}, I_x, I_y, I_α, J, L, x_α, P, $\overline{m}$, κ_{ax}, κ_{ay}, $\kappa_{a\psi}$, κ_{bx}, κ_{by}, $\kappa_{b\psi}$, S_{ax}, S_{ay}, S_{bx}, S_{by}, M_a, M_b, J_{ax}, J_{ay}, $J_{a\psi}$, J_{bx}, J_{by} and $J_{b\psi}$.
(2) Enter the trial value ω.
(3) Calculate the 28 dimensionless parameters and indices listed in Section 2.2.
(4) Calculate the values of χ, , λ, and δ including all 16 coefficients c_{ij} of matrix Eq. (22) and $\overline{x}_\alpha = x_\alpha/L$ as shown in Section 2.1 for the stability and vibration analyses in xz-plane. Then by making the determinant of the 4×4 matrix of Eq. (22)

equal to zero, the undamped natural frequencies ω can be determined directly for a given value of the applied axial force P, and the corresponding modes of vibration from Eqs. (16)–(17) once the eigen-vectors (values of F_1–F_4 for each frequency) are found in a standard manner. Alternatively, by making the determinant of the 4×4 matrix equal to zero the buckling load P_{cr} of the member AB can be also determined directly for a given value of ω. The static buckling loads can be also determined from Eq. (22) by making ω=0 in the eigen-value problem.

(5) Calculate the values of α, β, γ, $\overline{\alpha}$, $\overline{\beta}$, $\overline{\gamma}$, k_α, k_β, k_γ, g_α, g_β, g_γ including all 36 coefficients a_{ij} of matrix Eq. (52) listed in Section 2.2 for the vibration analyses in yz-plane. By making the determinant of the 6×6 matrix of Eq. (52) equal to zero, the undamped natural frequencies ω can be determined directly for a given value of the applied axial force P, and the corresponding modes of vibration from Eqs. (39)–(41) once the corresponding eigen-vectors (values of A_1–A_6 for each natural frequency) are found in a standard manner. Eq. (52) also represents the dynamic stability eigen-value problem of a singly symmetric Timoshenko beam-column with generalized end conditions when it bends in the yz-plane and twists about the z-axis. By making the determinant of the 6×6 matrix equal to zero the buckling load P_{cr} of the member AB can be determined directly for a given frequency ω. The static buckling loads can be also determined from Eq. (52) by making ω=0 in the eigen-value problem.

It is important to emphasize that Eqs. (22) and (52) which are based on the Haringx's approach (explained by Timoshenko and Gere [15]) is capable of capturing the phenomena of buckling under axial tension. This has been proven experimentally and analytically by Prof. Kelly at UC Berkeley [16] on elastomeric columns (see http://www.ce.washington.edu/em03/proceedings/papers/611.pdf) and discussed in detail by the author [8,9,18,21].

4. Illustrative examples

4.1. *Example 1: free vibration analysis of a 3D cantilever Timoshenko beam (effects of rotational stiffness at the base support on the natural frequencies)*

Determine the natural frequencies of a cantilever beam assuming the following properties: E_z=68.9 × 10^6 kN/m^2; G_y=26.5 × 10^6 kN/m^2; ρ=2711 kg/m^3; A= 3.08 × 10^{-4} m^2; I_x=9.26 × 10^{-8} m^4; E_zI_x=6.38 kN m^2; G_yA_{sy}=4081 kN; $G_{xy}J$=0.04346 kN m^2; $\overline{m}$=0.835 kg/m; I_α=0.501 × 10^{-3} kg m; x_α=0.0155 m and L=0.82 m. Analyze the following three cases: (1) P=0; (2) P=1.79 kN (tension); (3) P=−1.79 kN (compression) and also for (a) ρ_{ax}=1; (b) ρ_{ax}=0.75; (c) ρ_{ax}=0.5; (d) ρ_{ax}=0.25; and (e) ρ_{ax}=0. Compare the results with those presented by Banerjee [11] for case (a), clamped-free with ρ_{ax}=1.

Solution: The natural frequencies corresponding to the first four modes of vibration were calculated making the 6×6 determinant from the matrix [D] corresponding to Eq. (52) equal to zero. Table 1 shows the first four natural frequencies of

Table 1
Example 1: effects of the axial load and degree of fixity on the natural frequencies in the yz-plane of a cantilever beam-column (shear–bending–torsional coupling).

Mode	ρ_{ax}	**Natural frequency (Hz)**					
		P=0 (p^2=0)		P=1.79 kN (p^2=0.1886) Tension		P=−1.79 kN (p^2=−0.1886) Compression	
		Proposed model	Banerjee [11]	**Proposed model**	Banerjee [11]	**Proposed model**	Banerjee [11]
1	1	62.34	62.34	64.58	64.59	59.98	59.97
	0.75	54.44		56.91		51.81	
	0.50	44.51		47.38		41.40	
	0.25	31.32		35.11		26.95	
	0	115.22		15.51		114.17	
2	1	129.9	129.9	131.6	131.6	128.1	128.1
	0.75	125.2		126.6		123.7	
	0.50	121.2		122.4		119.9	
	0.25	117.9		119.0		116.7	
	0	228.0		116.2		223.9	
3	1	259.2	259.2	262.4	262.4	256.0	256.0
	0.75	248.6		252.0		245.1	
	0.50	240.0		243.7		236.4	
	0.25	233.3		237.1		229.4	
	0	414.8		231.9		409.4	
4	1	418.9	424.6	424.6	424.6	413.1	413.1
	0.75	417.9		423.5		412.2	
	0.50	416.9		422.5		411.2	
	0.25	415.9		421.3		410.3	
	0	492.2		420.2		489.1	

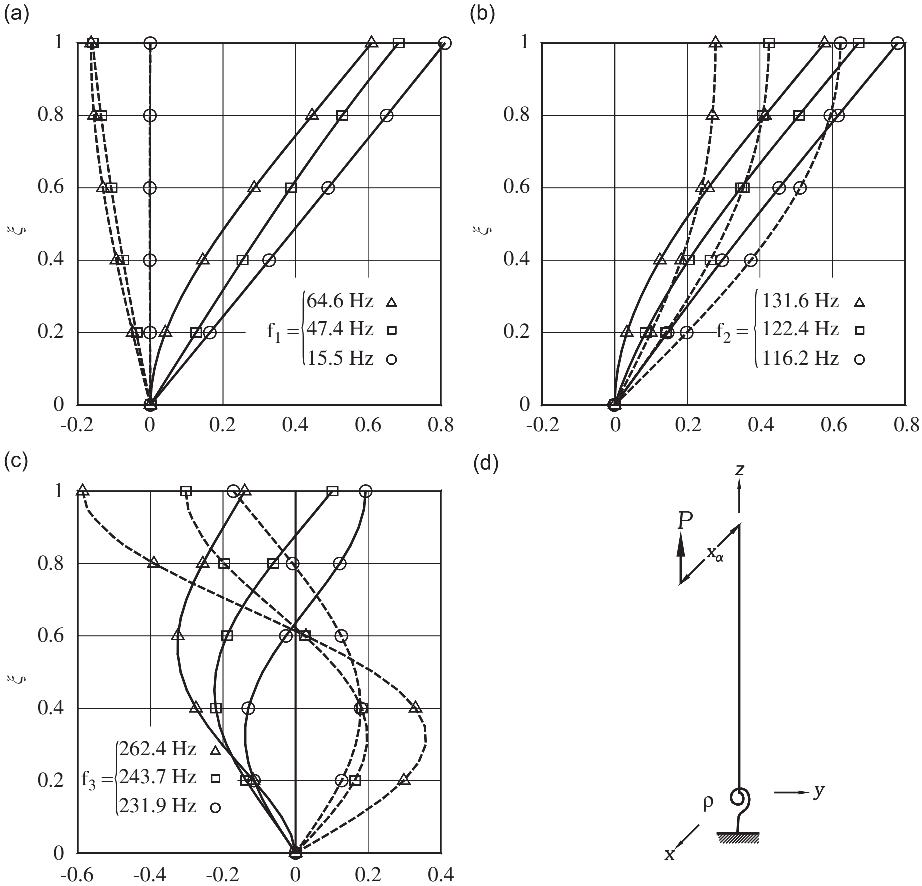

Fig. 2. Example 1: (a) first-; (b) second-; and (c) third-modal shapes of an axially loaded cantilever Timoshenko beam-column with p^2=0.1886, r^2=0.00047, s^2=0.0023 and for three different values of ρ: V(______), $x_\alpha\Psi$(— — —) for ρ=1; V(———), $x_\alpha\Psi$(− − − −) for ρ=0.5; V(———), $x_\alpha\Psi$ (− − − −) for ρ=0; and (d) structural model.

the cantilever beam with three cases different of load and five rotational stiffness κ_{ax}, calculated for several values of ρ_a with the following equation:

$$\rho_{ax} = \frac{1}{1 + 3(E_z I_x/L)/\kappa_{ax}}, \tag{53}$$

where ρ_a is called the fixity factor. Notice that ρ_a is more convenient to use in the analysis of structures with semirigid connections since it varies from 0 (for perfectly hinged connections) to 1 (for perfectly clamped connections), whereas the rotational stiffness κ_a varies from 0 to ∞.

The obtained results for the case (a) clamped-free with ρ=1 were compared with those reported by Banerjee [11] showing excellent agreement. Figs. 2 and 3 show the shapes corresponding to the first three modes of vibration (translation V and torsion $x_\alpha\Psi$) of the cantilever beam-column for different values of ρ under tension and compression, respectively. Notice that the high modes of vibration are more sensitive to the degree of fixity at the base.

4.2. Example 2: free vibration analysis of a 3D cantilever Timoshenko beam (effects of torsional stiffness at the base)

Determine the natural frequencies of a cantilever beam assuming the following properties: E_z=2.1 × 10^8 kN/m^2; G_y=78.94736 × 10^6 kN/m^2; ρ=7800 kg/m^3; A=9 × 10^{-4} m^2; I_x=19.638 × 10^{-8} m^4; E_zI_x=41.241669 kN m^2; G_yA_{sy}=35,530 kN; $G_{xy}J$=2.368421 kN m^2; $\overline{m}$=7.02 kg/m; I_α=3.237 × 10^{-3} kg m; x_α=0.0111 m; and L=1 m. Analyze the following three cases: (1) P=15 kN; (2) P=−15 kN; and (3) P=0 and also for (a) $\kappa_{a\psi}$=∞; (b) $\kappa_{a\psi}$=9GJ/L; (c) $\kappa_{a\psi}$=3GJ/L; (d) $\kappa_{a\psi}$=GJ/L; and (e) $\kappa_{a\psi}$=0. Compare the results with those reported by Viola et al. [14] for case (a) clamped-free with $\kappa_{a\psi}$=∞.

Solution: The natural frequencies corresponding to the first four modes of vibration were calculated making the 6 × 6 determinant of matrix [D] of Eq. (52) equal to zero. Table 2 lists the natural frequencies for three different load cases and five rotational stiffness $\kappa_{a\psi}$. The obtained results for case (a) clamped-free with $\kappa_{a\psi}$=∞ is compared with those reported by Viola et al. [14]. The first three modes of vibration are shown in Fig. 4.

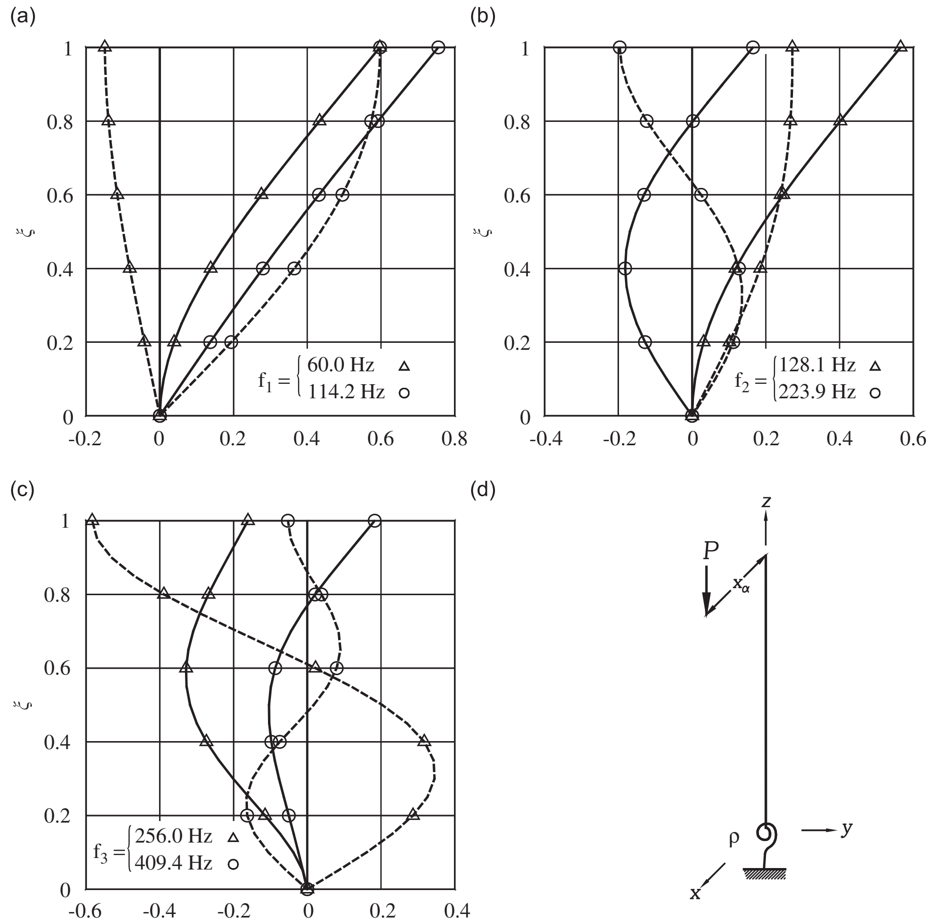

Fig. 3. Example 1: (a) first-; (b) second-; and (c) third-modal shapes of an eccentrically loaded cantilever Timoshenko beam-column for two values of ρ: V(———), $x_\alpha\Psi$(— — — —) for ρ=1; and V(———), $x_\alpha\Psi$(— — — —) for ρ=0; and (d) structural model.

The stability and free vibration analyses in the *xz*-plane of a perfectly clamped cantilever Timoshenko beam-column with $\kappa_{by} = S_{bx} = M_a = M_b = P = 0$ and S_{ax}=R_{ay}=∞ can be obtained from the 4×4 matrix of Eq. (22) resulting in the following characteristic equation:

$$2 + \left(\frac{\eta}{\chi} - \frac{\chi}{\eta}\right)\sin\chi\sinh\eta - \left(\frac{\lambda\chi}{\delta\eta} + \frac{\delta\eta}{\lambda\chi}\right)\cos\chi\cosh\eta = 0, \tag{54}$$

where $\lambda = (-\chi^2 + b_u^2 s_u^2)/\chi$; and $\delta = (\eta^2 + b_u^2 s_u^2)/\eta$.

The natural frequencies for case (a) (clamped-free, ρ_{ay}= 1) listed in Table 3 were calculated using Eq. (54). The buckling loads values were calculated using the following characteristic equation:

$$2 + \left(\frac{\eta}{\chi} - \frac{\chi}{\eta}\right)\sin\chi\sinh\eta - \left(\frac{\lambda\chi}{\delta\eta} + \frac{\delta\eta}{\lambda\chi}\right)\cos\chi\cosh\eta = \lambda\chi\frac{p_u^2}{b_u^2}, \tag{55}$$

where

$$\lambda = \frac{-\chi^2 + b_u^2 s_u^2}{\chi(1 - p_u^2 s_u^2)} \quad \text{and} \quad \delta = \frac{\eta^2 + b_u^2 s_u^2}{\eta(1 - p_u^2 s_u^2)}.$$

The corresponding vibration mode shape from Eq. (16):

$$U(\xi) = F_3(\cos\chi\xi - \cosh\eta\xi) + F_4\left(\sin\chi\xi + \frac{\lambda}{\delta}\sinh\eta\xi\right), \tag{56}$$

Table 2
Example 2: effects of axial load and torsional fixity on the natural frequencies in the *yz*-plane of a cantilever beam-column (shear–bending–torsional coupling).

Mode	$\kappa_{a\psi}$	Natural frequency (Hz)					
		P=0 (p^2=0)		P=15 kN (p^2=0.3637) Tension		P=−15 kN (p^2=−0.3637) Compression	
		Proposed model	Viola et al. [14]	**Proposed model**	Viola et al. [14]	**Proposed model**	Viola et al. [14]
1	∞	42.538	42.485	45.331	45.270	39.483	39.435
	$9GJ/L$	42.497		45.281		39.451	
	$3GJ/L$	42.414		45.178		39.385	
	GJ/L	42.147		44.848		39.177	
	0	46.717		49.823		43.327	
2	∞	233.548	233.546	235.236	235.239	231.732	231.723
	$9GJ/L$	213.215		214.234		212.120	
	$3GJ/L$	180.648		181.233		180.031	
	GJ/L	130.710		131.109		130.303	
	0	266.253		269.352		263.104	
3	∞	276.750	276.737	278.590	278.583	274.988	274.970
	$9GJ/L$	272.099		274.521		269.704	
	$3GJ/L$	269.200		271.985		266.397	
	GJ/L	267.412		270.398		264.387	
	0	459.383		460.355		458.409	
4	∞	632.144	632.138	634.712	634.735	629.558	629.523
	$9GJ/L$	592.006		593.922		590.071	
	$3GJ/L$	540.781		542.127		539.422	
	GJ/L	494.337		495.416		493.253	
	0	726.330		729.015		723.633	

where

$$F_3 = p_u^2 \overline{x}_\alpha \frac{\dfrac{\lambda}{\delta}[\eta + (p_u^2 s_u^2 - 1)\delta]\cosh\eta + [\chi - (p_u^2 s_u^2 - 1)\lambda]\cos\chi}{2 + \left(\dfrac{\eta}{\chi} - \dfrac{\chi}{\eta}\right)\sin\chi\sinh\eta - \left(\dfrac{\lambda\chi}{\delta\eta} + \dfrac{\delta\eta}{\lambda\chi}\right)\cos\chi\cosh\eta - \lambda\chi\dfrac{p_u^2}{b_u^2}}.$$

In the case of clamped-free Euler–Bernoulli beam [2,18] the first three natural frequencies are

$$\omega_1 = \frac{(1.875)^2}{L^2}\sqrt{\frac{E_z I_y}{\overline{m}}};\quad \omega_2 = \frac{(4.694)^2}{L^2}\sqrt{\frac{E_z I_y}{\overline{m}}};\quad \omega_3 = \frac{(7.855)^2}{L^2}\sqrt{\frac{E_z I_y}{\overline{m}}};$$

and for a clamped-free shear beam [2], the n-frequency is given by (Table 4)

$$\omega_n = \frac{(2n-1)\pi}{2L}\sqrt{\frac{G_x A_{sx}}{\overline{m}}}.$$

The results obtained using Eq. (54) are compared with results using these formulas in Table 5.

Fig. 4 shows the calculated modal shapes corresponding to the first three modes of vibration and the corresponding variation of frequencies f against the axial load P for different values of the stiffness of the torsional end restraint $\kappa_{a\psi}$ (=∞, GJ/L, and zero).

4.3. Example 3: stability and dynamic analyses of a composite column made of E-glass fiber

Analyze a 200 × 200 × 10 mm composite column tested by Roberts [17] but partially restrained at both ends with the following properties: E_z=1.886 × 10^7 kN/m^2; G_x=2.671 × 10^6 kN/m^2; (E-glass fiber) ρ=2550 kg/m^3; $\overline{m}$=14.79 kg/m; L=4.5 m; A=5.8 × 10^{-3} m^2; A_{sx}=2 × 10^{-3} m^2; I_y=4.16 × 10^{-5} m^4; S_{ax}=5000 kN/m; S_{bx}=25,000 kN/m; and ρ_{ay}=ρ_{by}=ρ. Determine the static critical loads and natural frequencies.

Solution: The static critical loads (i.e. assuming ω=0) corresponding to the first three buckling modes in the *xz*-plane for four different cases of fixity factors ρ_{ay}=ρ_{by}=ρ=1, 0.75, 0.5, and 0.25 are listed in Table 6. Notice that the compressive buckling loads are more sensitive to the magnitude of the end bending restraints than those of columns under tension.

Table 7 lists the axial loads corresponding to the first three modes of buckling in the *xz*-plane for the particular case of perfectly pinned ends (i.e., ρ_{ay}=ρ_{by}=0 and S_{ax}=S_{bx}=∞) using the proposed method and that by Arboleda-Monsalve et al. [20]. The two methods yield very similar results. Notice that the value reported by Roberts [17] of P_{cr}=358 kN in compression compares very well with the value of 358.5 kN obtained with the proposed method. The last two columns of Table 7 and the results listed in Table 8 also show that the proposed method is capable of capturing the critical loads and

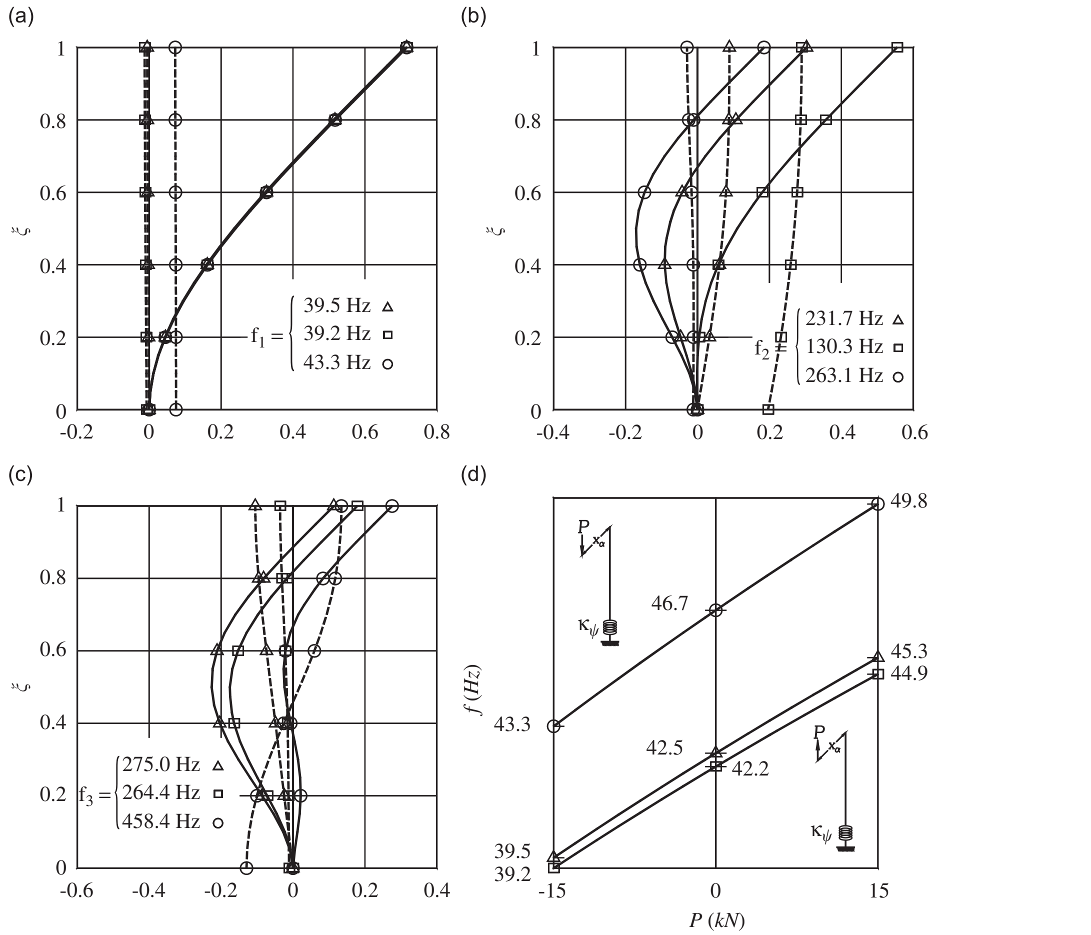

Fig. 4. Example 2: (a) first-; (b) second-; and (c) third-modal shapes of an axially loaded cantilever Timoshenko beam-column with p^2=−0.3637, r^2=0.000218, s^2=0.00116: V(———), $x_\alpha\Psi$(— — — —) for $\kappa_{a\psi}=\infty$; V(———), $x_\alpha\Psi$(— — — —) for $\kappa_{a\psi}=GJ/L$; V(———), $x_\alpha\Psi$(— — — —) for $\kappa_{a\psi}$=0; and (d) variation of frequency f against the axial load P for different values of the stiffness of the torsional end restraint: (———) for $\kappa_{a\psi}=\infty$; (———) for $\kappa_{a\psi}=GJ/L$; and (———) for $\kappa_{a\psi}$=0.

natural frequencies

$$\left[\omega_n = \frac{(n\pi)^2}{L^2}\sqrt{\frac{E_z I_y}{\overline{m}}}\right]$$

of a pinned–pinned Euler–Bernoulli column (as $G_x A_{sx} \to \infty$).

Table 9 shows the values of the natural frequencies of a partially restrained column for five different values of $\rho_{ay}=\rho_{by}=\rho$=1, 0.75, 0.5, 0.25, 0, and S_{ax}=15,000 kN/m, S_{bx}=25,000 kN/m and three different values of P=0, 5 kN (tension) and −5 kN (compression).

Fig. 5 shows the variations of the first-mode natural frequency in the xz-plane of the composite column with the applied axial load P for four different values of $\rho_{ay}=\rho_{by}=\rho$=1, 0.75, 0.5, 0.25 and 0. Notice that the first-mode natural frequency: (1) decreases with the magnitude of the compressive axial load and when the fixity factors are reduced; (2) increases with the magnitude of the tension axial load up reaching a peak located at a P value slightly less than P_{cr} and then decreases rapidly to zero at P_{cr} in tension; and (3) the maximum frequency occurs at P=5340 kN and is not affected by the stiffness of the rotational restraints.

4.4. Example 4: free vibration of a cantilever Timoshenko beam-column (sensitivity study)

A sensitivity study was carried out on the effects of axial load (tension and compression), axial load eccentricity, and degree of fixity at the base support on the natural frequencies of a Timoshenko beam-column in the yz-plane (see Fig. 6d).

Figs. 6 and 7 show the variations of the first-mode natural frequency as the applied axial-load varies (from compression to tension) and as the combined parameter s^2b^2/a^2 varies, respectively for five different values of the axial-load eccentricity

Table 3
Example 2: effects of axial load and degree of fixity on the natural frequencies in the *xz*-plane cantilever beam-column assuming E_zI_y=22.575 kN m^2 and G_xA_{sx}=32,897 kN.

Mode	ρ_{ay}	Natural frequency (Hz)		
		P=0 ($p_u^2=0$)	P=15 kN ($p_u^2=0.6644$) Tension	P=$-$15 kN ($p_u^2=0.6644$) Compression
1	1	31.674	35.351	27.346
	0.75	26.329	30.082	21.754
	0.50	20.652	24.783	15.226
	0.25	14.048	19.202	4.523
	0	138.387	12.664	132.973
2	1	196.324	200.676	191.859
	0.75	171.536	176.034	166.903
	0.50	156.101	160.844	151.194
	0.25	145.751	150.732	140.575
	0	442.675	143.576	438.363
3	1	540.344	544.096	536.566
	0.75	486.923	490.843	482.971
	0.50	463.420	467.502	459.300
	0.25	450.634	454.827	446.400
	0	905.433	446.944	901.496
4	1	1033.800	1037.400	1030.200
	0.75	953.330	957.060	949.585
	0.50	926.242	930.073	922.395
	0.25	913.119	917.004	909.217
	0	1508.900	909.352	1505.200

Table 4
Example 2: effects of degree of fixity on buckling Loads[a] in the *xz*-plane.

Mode[a]	ρ_{ay}	P_{cr} Proposed model (kN)	P_e Euler load (kN)	P_{cr}/P_e
1	1	55.6	55.7	0.998
	0.75	45.1		
	0.50	32.1		
	0.25	16.7		
	0	221.3		
2	1	493.9	501.3	0.985
	0.75	406.5		
	0.50	324.3		
	0.25	262.8		
	0	868.3		
3	1	1338.1	1392.5	0.961
	0.75	1125.5		
	0.50	985.10		
	0.25	910.30		
	0	1896.0		

[a] *Note*: Although the lowest critical buckling load is of main practical importance, the higher buckling modes should be taken in the context of duality between free vibration and buckling problems.

Table 5
Example 2: natural frequencies for Euler–Bernoulli and shear beams (calculated using proposed model against those obtained from classical formulas).

Mode	Natural frequency (Hz)			
	Proposed model $G_xA_{sx}\to\infty$	Euler–Bernoulli beam	Proposed model $E_zI_y\to\infty$	Shear beam
1	31.72	31.72	541.19	541.19
2	198.49	198.86	1623.57	1623.57
3	554.29	556.87	2705.95	2705.95

Table 6
Example 3: effects of degree of fixity on buckling loads.

Mode	ρ_{ay}=ρ_{by}	$\boldsymbol{P_{cr}}$ **(kN)** Compression	$\boldsymbol{P_{cr}}$ **(kN)** Tension
1	1	1241.7	5717.5
	0.75	906.6	5597.6
	0.50	653.3	5491.3
	0.25	479.9	5406.2
	0	358.5	5698.5
2	1	2145.6	6581.7
	0.75	1725.7	6246.6
	0.50	1483.7	5993.3
	0.25	1337.7	5819.9
	0	1241.7	6581.7
3	1	3640.2	7795.3
	0.75	2927.6	7207.7
	0.50	2608.2	6863.4
	0.25	2461.6	6684.1
	0	2381.4	7721.4

Table 7
Example 3: buckling loads (pinned–pinned column).

Mode	$\boldsymbol{P_{cr}}$ **(kN)** Compression		$\boldsymbol{P_{cr}}$ **(kN)** Tension		**Euler–Bernoulli column**	
	Proposed model	Arboleda et al. [19]	**Proposed model**	Arboleda et al. [19]	**Proposed model** $G_xA_{sx}\to\infty$	$\boldsymbol{P_e}$
1	358.5	358.0	5698.5	5697.7	382.6	382.6
2	1241.7	1239.5	6581.7	6579.6	1530.4	1530.4
3	2381.4	2379.6	7721.4	7719.3	3443.4	3443.4

Table 8
Example 3: Natural frequencies calculated using proposed model-versus-classical formulas for Euler–Bernoulli beam.

Mode	**Natural frequency (Hz)**		
	Proposed model ($G_xA_{sx}\to\infty$)	**Euler–Bernoulli beam**	**Error (%)**
1	17.84	17.87	0.2
2	70.99	71.48	0.7
3	158.37	160.84	1.5

Table 9
Example 3: effects of degree of fixity on the natural frequencies in the *xz*-plane of a partially restrained PFRP column.

Mode	ρ_{ay}=ρ_{by}	**Natural frequency (Hz)**		
		P=0 (p^2=0)	P=5 kN (p^2=0.1290) Tension	P=−5 kN (p^2=−0.1290) Compression
1	1	32.36	32.41	32.31
	0.75	26.60	26.66	26.53
	0.50	22.54	22.63	22.46
	0.25	19.44	19.54	19.34
	0	16.91	17.03	16.80
2	1	70.74	70.80	70.67
	0.75	65.50	65.58	65.42
	0.50	62.36	62.45	62.26
	0.25	60.26	60.36	60.16
	0	58.76	58.86	58.66
3	1	115.85	115.93	115.77
	0.75	112.82	112.91	112.73
	0.50	111.39	111.48	111.30
	0.25	110.56	110.65	110.46
	0	110.02	110.11	109.92

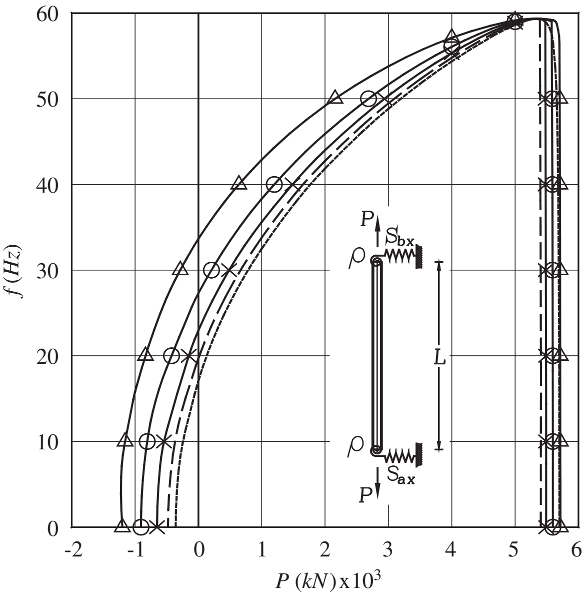

Fig. 5. Example 3: Variation of the first-mode natural frequency f with the applied axial load P (+ tension) for five different values of the fixity factor ρ: (———) for ρ=1; (———) for ρ=0.75; (—×—) for ρ=0.5; (- - -) for ρ=0.25; (—) for ρ=0 and assuming that both ends are partially restrained with S_{ax}=5000 kN/m and S_{bx}=25,000 kN/m.

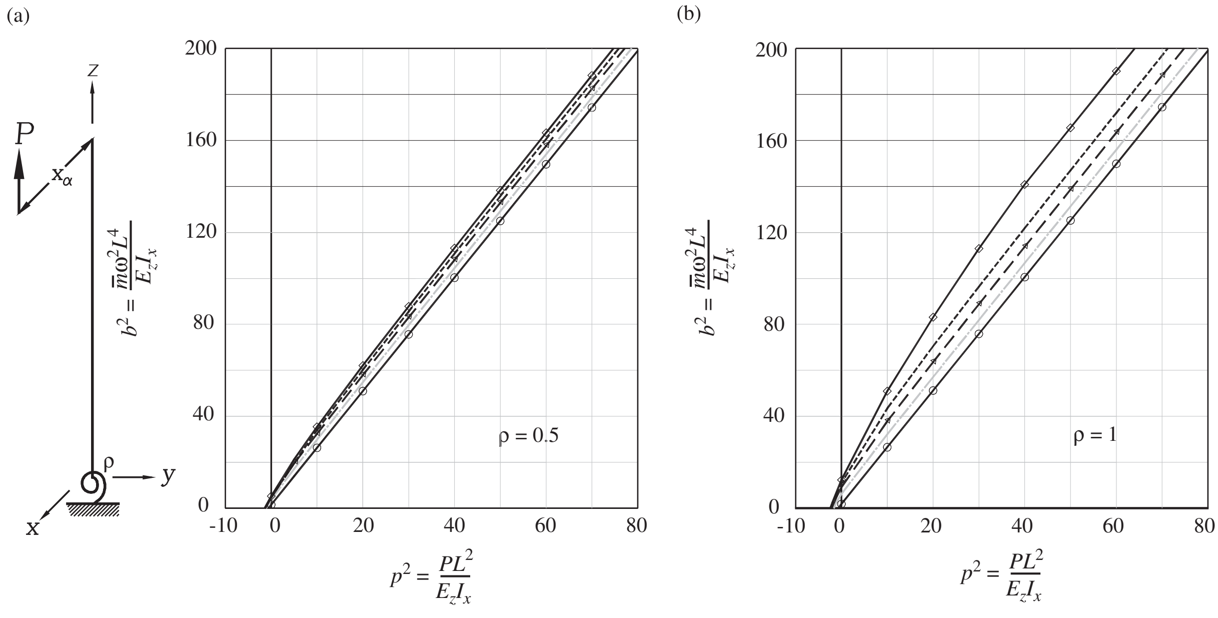

Fig. 6. Variation of the first-mode natural frequency parameter b^2 for a cantilever beam-column with the applied axial-load parameter p^2 for five different values of the eccentricity parameter c^2 [=0.05 (———); .25 (- - -); 0.50 (— △ —); .75 (- - -); and 1 (—◇—)] for two different values of the fixity factor ρ: (a) ρ=0.5; and (b) ρ=1 assuming a bending-to-shear stiffness parameter s^2=1/1000.

parameter c^2 and for two different values of fixity ρ (0.5 and 1) at the base of the cantilever. Notice that: (1) $b^2s^2/a^2 = \overline{m}G_{xy}J/I_\alpha G_y A_{sy}$ is the combined torsional-shear parameter; (2) the eccentricity parameter $c^2 = 1 - \overline{m}x_\alpha^2/I_\alpha$ varies from 1 (zero eccentricity) to 0 (maximum eccentricity); (3) $a^2 = I_\alpha\omega^2L^2/G_{xy}J$ and $b^2 = \overline{m}\omega^2L^4/E_zI_x$ (frequency parameters), $p^2 = PL^2/E_zI_x$ (axial-load parameter) and $s^2 = E_zI_x/G_yA_{sy}L^2$ (bending-to-shear stiffness parameter).

Based on the results indicated by Figs. 6 and 7 it is concluded that the first-mode frequency in the yz-plane increases: (1) almost linearly as the axial load is increased in tension, but it is reduced by compressive axial loads; (2) with the degree of fixity at the base ρ but it is reduced by the torsional effects caused by the eccentricities (of the axial load and those of the masses); and (3) low shear stiffness always have the effect of reducing the natural frequencies, whereas tension axial loads increase substantially the natural frequencies.

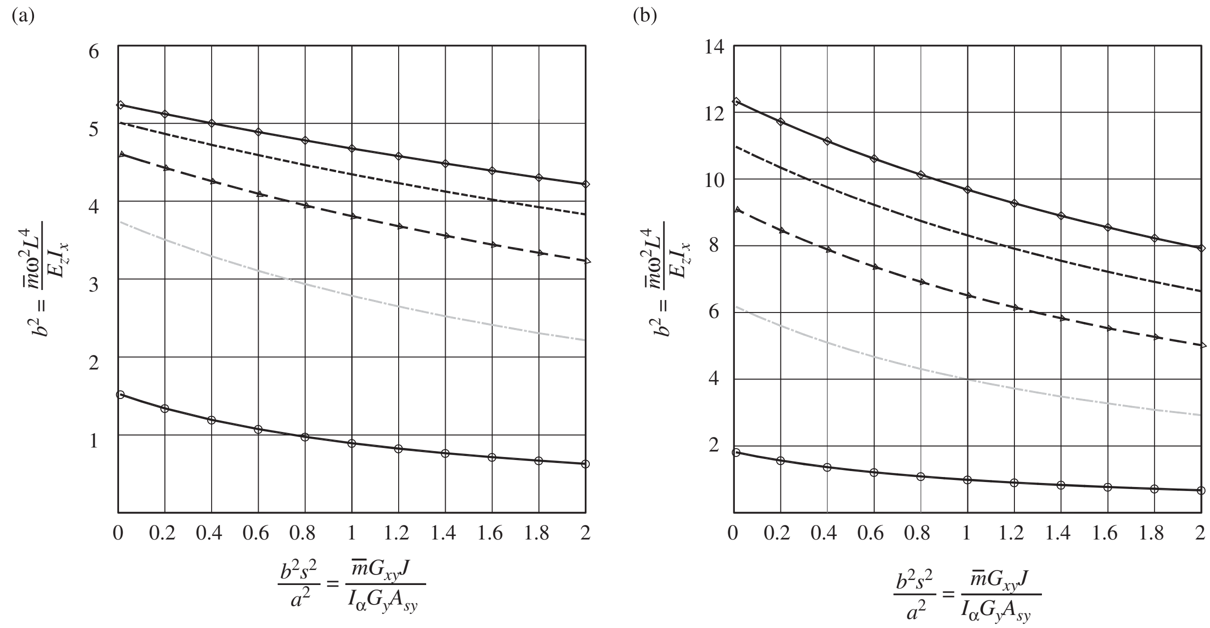

Fig. 7. Variation of the first-mode natural frequency parameter b^2 for a cantilever beam with b^2s^2/a^2 for five different values of the eccentricity parameter c^2 [=0.05 (———); 0.25 (- - -); 0.50 (— △ —); 0.75 (- - -); and 1 (—◇—)] for two different values of the fixity factor ρ: (a) ρ=0.5; and (b) ρ=1 assuming an axial load parameter p^2=0.

5. Summary and conclusions

The stability and free vibration analyses (i.e., lateral buckling loads, natural frequencies and modal shapes) of an orthotropic singly symmetrical Timoshenko beam-column with generalized support conditions (i.e., with semirigid flexural and torsional restraints and lateral bracings about and along the principal axes of bending as well as lumped masses at both ends) subjected to an eccentric end axial load are derived in a classic manner. The proposed model include the three dimensional coupling effects of all deformations (i.e., bending and shear about and along the principal axes of bending as well as those caused by pure torsion along the axis of the member), a uniform mass distributed along its span, the applied eccentric axial load (tension or compression) at both ends, the three dimensional inertias (translational, rotational and torsional) of all masses considered. The effects of the shear force component induced by the applied axial force as the member bends about each of its principal axes have been included as suggested by Haringx [16–18]. However, the effects of warping torsion, torsional stability and combined bending–torsional buckling are not included in this study since it would require a much more complex model. To include these effects the model must include not only the three dimensional couplings between "mixed" torsion and biaxial bending as shown by Curver [19] but also extremely complex semirigid conditions to resist warping torsion at both ends. Consequently, the proposed method is not capable of capturing the phenomena of torsional buckling or combined bending–torsional buckling. However, the proposed model is more general than any other model available in the technical literature including that presented by Banerjee [11] and Aristizabal-Ochoa [18], since it includes generalized 3D support conditions, orthotropic material properties, the effects of the shear force components induced by the applied axial force as the member bends about both principal axes (according to the "modified" shear equation or Haringx approach), and 3D end masses. All these additional considerations and effects are important in the analysis and design of buildings and beam structures, particularly when made of materials with low shear moduli.

The stability and free vibration analyses of a singly symmetrical orthotropic Timoshenko beam-column as presented in this paper depend on 34 variables: E_z, G_x, G_y, G_{xy}, A, A_{sx}, A_{sy}, I_x, I_y, I_α, J, L, x_α, P, $\overline{m}$, ω, κ_{ax}, κ_{ay}, $\kappa_{a\psi}$, κ_{bx}, κ_{by}, $\kappa_{b\psi}$, S_{ax}, S_{ay}, S_{bx}, S_{by}, M_a, M_b, J_{ax}, J_{ay}, $J_{a\psi}$, J_{bx}, J_{by} and $J_{b\psi}$. However, these variables can group into 28 nondimensional parameters and indices. The proposed equations have the capability of modeling the simplified beams, and beam-columns cases like those based on the following classic theories: (1) Bernoulli–Euler; (2) Rayleigh; (3) Timoshenko; (4) shear beam-column all with or without axial load. In addition, the proposed model is capable of determining: (1) the static and dynamic stability of 3D and 2D beam-columns with or without the simultaneous bending and shear deformations; and (2) the effects of an eccentric end axial load (tension or compression) on the natural frequencies of Timoshenko beam-columns with generalized end conditions. The proposed model also captures the phenomena of modal interchanges in beams and beam-columns with soft end connections (i.e., when the second-mode of vibration becomes the first mode and similarly with the upper modes) as shown in Example 2.

Analytical results obtained in this study indicate that: (1) the critical loads and natural frequencies increase substantially by increasing the magnitude of the bending, torsional and lateral restraints at both ends; (2) compressive axial loads and shear and torsional deformations always have the effect of reducing the natural frequencies, particularly those of the lower modes of vibration, whereas tension axial loads (slightly lower than its P_{cr} in tension) increase substantially the natural frequencies and lateral stability of beam-columns; and (3) the coupling effects among all deformations (bending, shear and torsional) must not be ignored in the stability and vibration analyses of singly symmetry beam-columns as described by Eqs. (22) and (52).

Further research on the effects of "mixed" torsion and the corresponding semirigid conditions at the supports capable to capture lateral torsional buckling in symmetric and nonsymmetric Timoshenko beam-columns with generalized boundary conditions is needed.

Acknowledgments

The research presented in this paper was carried out at the National University of Colombia, School of Mines at Medellin. The authors want to express their appreciation to DIME for the financial support and to Prof. Gabriel Gomez for his encouragement.

References

[1] W.T. Thomson, *Theory of Vibration with Applications*, Prentice-Hall, Englewood Cliffs NJ, 1972, pp. 275–276 (Chapter 8).
[2] R.D. Blevins, *Formulas for Natural Frequency and Mode Shape*, Van-Nostrand Reinhold, New York, 1979, pp. 171–176 (Chapter 8).
[3] G.V. Berg, *Elements of Structural Dynamics*, Prentice-Hall, Englewood Cliffs, NJ, 1989.
[4] M. Paz, *Structural Dynamics: Theory and Computation*, third ed., Van-Nostrand Reinhold, New York, 1991, pp. 201–296 (Chapters 9–13).
[5] R.W. Clough, J. Penzien, *Dynamics of Structures*, second ed., McGraw-Hill, New York, 1993 (Chapter 18).
[6] A. Chopra, *Structural Dynamics*, second ed., McGraw-Hill, New York, 1998, p. 628 (Chapter 26).
[7] J. Dario Aristizabal-Ochoa, Timoshenko beam-column with generalized end conditions and nonclassical modes of vibration of shear beams, *Journal of Engineering Mechanics, ASCE* 130 (10) (2004) 1151–1159.
[8] J. Dario Aristizabal-Ochoa, Static and dynamic stability of uniform shear beam-columns under generalized boundary conditions, *Journal of Sound and Vibration* 307 (2007) 69–88.
[9] J. Dario Aristizabal-Ochoa, Dynamic modal analysis and stability of cantilever shear buildings: importance of moment equilibrium, *Journal of Engineering Mechanics, ASCE* 133 (7) (2007) 735–747.
[10] J.R. Banerjee, S. Guo, W.P. Howson, Exact dynamic stiffness matrix of a bending–torsion coupled beam including warping, *Computers & Structures—Elsevier* 59 (4) (1996) 613–621.
[11] J.R. Banerjee, Explicit modal analysis of an axially loaded Timoshenko beam with bending torsion coupling, *Journal of Applied Mechanics—ASME* (2000) 307–313.
[12] Li Jun, Shen RongyingJin Xianding, Coupled bending and torsional vibration of axially loaded Bernoulli–Euler beams including warping effects, *Applied Acoustics* 65 (2004) 153–170.
[13] B. Rafezy, W.P. Howson, Exact dynamic stiffness matrix of a three-dimensional shear beam with doubly asymmetric cross-section, *Journal of Sound and Vibration* 289 (2006) 938–951.
[14] E. Viola, P. Ricci, M.H. Aliabadi, Free vibration analysis of axially loaded cracked Timoshenko beam structures using dynamic stiffness method, *Journal of Sound and Vibration* 304 (2007) 124–153.
[15] S.P. Timoshenko, J.M. Gere, *Theory of Elastic Stability Engineering Societies Monographs*, McGraw-Hill, New York, 1961 pp. 134.
[16] J.M. Kelly, Tension buckling in multilayer elastomeric bearings, *Journal of Engineering Mechanics* 129 (12) (2003) 1363–1368 (Discussion by J. Dario Aristizabal-Ochoa, 131 (1) (2005) 106–108).
[17] T.M. Roberts, Influence of shear deformation on buckling of pultruded fiber reinforced plastic profiles, *Journal of Composites for Construction—ASCE* (11) (2002) 241–248.
[18] J. Dario Aristizabal-Ochoa, Tension and compression stability and second-order analyses of three-dimensional multicolumn systems: effects of shear deformations, *Journal of Engineering Mechanics ASCE* 133 (1) (2007) 106–116.
[19] C.G. Curver, Exact solution of the biaxial bending equations, *Journal of the Structural Division, ASCE* 92 (2) (1966) 63–83.
[20] L.G. Arboleda-Monsalve, D.G. Zapata-Medina, J. Dario Aristizabal-Ochoa, Stability and natural frequencies of a weakened Timoshenko beam-column with generalized end conditions under constant axial load, *Journal of Sound and Vibration* 307 (2007) 89–112.
[21] J. Dario Aristizabal-Ochoa, Slope-deflection equations for stability and second-order analysis of Timoshenho beam-column structures with semi-rigid connections, *Engineering Structures* 30 (9) (2008) 2517–2527 (Clossure: Engineering Structures 30 (11) (2008) 3394–3395).